CORTICAL EEG SOURCE LOCALIZATION OF FOCAL EPILEPSY

by

Wisal Elfatih Mohamed Siyam

A Thesis presented to the Faculty of the
American University of Sharjah
College of Engineering
In Partial Fulfillment
of the Requirements
for the Degree of

Master of Science in
Electrical Engineering

Sharjah, United Arab Emirates

November 2017

© 2017 Wisal Elfatih Mohamed Siyam. All rights reserved.

Approval Signatures

We, the undersigned, approve the Master's Thesis of Wisal Elfatih Mohamed Siyam

Thesis Title: Cortical EEG Source Localization of Focal Epilepsy.

Signature	**Date of Signature** (dd/mm/yyyy)
_____	_____
Dr. Hasan Mir Associate Professor, Department of Electrical Engineering Thesis Advisor	
_____	_____
Dr. Hasan Al-Nashash Professor, Department of Electrical Engineering Thesis Co-Advisor	
_____	_____
Dr. Amer Zakaria Assistant Professor, Department of Electrical Engineering Thesis Committee Member	
_____	_____
Dr. Gerassimos Barlas Professor, Department of Computer Science and Engineering Thesis Committee Member	
_____	_____
Dr. Nasser Qaddoumi Head, Department of Electrical Engineering	
_____	_____
Dr. Ghaleb Husseini Associate Dean for Graduate Affairs and Research College of Engineering	
_____	_____
Dr. Richard Schoephoerster Dean, College of Engineering	
_____	_____
Dr. Mohamed El-Tarhuni Vice Provost for Graduate Studies	

Acknowledgement

First of all, I would like to thank ALLAH for blessing me and giving me the opportunity to study and complete my graduate studies at AUS. Then, I want to thank AUS for supporting me with a full Graduate Assistanship during my master study. Also, I want to thank the head of Electrical Engineering Department, Dr. Naser Qaddoumi, for his support and for being like a father to me. I would also express my gratitude to my kind advisors, Dr. Hasan Mir and Dr. Hasan Al-Nashash for their continuous guidance, help, and support. Thank you professors for being the best advisors.

I would like to thank my mother for standing by my side all the time. Also thank you my brother and sisters for having faith in me.

I would like to thank my dear husband, Mohamed Anass, who supported me throughout my graduate studies at AUS and for making my difficult days easier. Also, many thanks for my baby boy, Ammar, for teaching me how to be patient, strong and determined.

Special thanks to Dr. Mahmoud Hasan at the laboratory of Signal and Image processing in France for helping and sharing with us his experience in localizing epileptogenic spikes. And to Dr. Mohamed Kaylani from neurology ward at Rashid Hospital for providing us with patients' EEG recordings and medical reports necessary for our work.

Abstract

Brain source localization allows us to localize different brain regions that are activated during neural activity. Several imaging modalities can be used for recording neural activity and are essential in clinical applications. One of these clinical applications is epilepsy diagnosis and localization. Structural or/and functional imaging techniques are used for patients to investigate epilepsy, classify seizures, and in pre-surgical evaluation. This report summarizes the most common imaging techniques for epilepsy diagnosis. It will then make use of electroencephalography (EEG) readings to localize epileptogenic regions in the brain, as it is a noninvasive technique with high temporal resolution. In addition, EEG requires low-cost hardware when compared with the other modalities such as functional Magnetic Resonance Imaging (fMRI), Positron Emission Tomography (PET), and Single Photon Emission Computed Tomography (SPECT). Moreover, the most common source models are discussed along with the used signal processing based techniques for source localization. In this work, distributed sources dipole model algorithms including the SAFFIRE and sLORETA are discussed and applied to simulated epileptic spikes. Upon examination of these algorithms, their potential in epilepsy source localization was proven with relatively low localization errors of 6.25 cm and 3.55 cm for sLORETA and SAFFIRE algorithms respectively. The SAFFIRE algorithm performance is investigated on epilepsy real data where the localized epileptogenic foci were consistent to the suggested locations by neurologists. Furthermore, the effect of reducing the number of electrodes on the source localization error was investigated on simulated epileptic spikes. The source localization error increased by 2.18 cm when reducing the number of electrodes from 256 down to 128. Then it increased by 3.7 mm when going from 128 electrodes to 64 electrodes. In conclusion, the localization error is inversely proportional to the number of electrodes used for recording brain potentials.

Search Terms: ***Epilepsy, EEG, Brain source model, Brain source localization, inverse problem, SAFFIRE algorithm.***

Table of Contents

List of Figures

Chapter 1. Introduction

1.1 Brain Source Localization

Brain Source Localization techniques are becoming important in clinical applications due to their role in improving the understanding and treatment of serious neurological and neurophysiological disorders such as Epilepsy, Parkinson's Disorder, Schizophrenia, and Alzheimer [1, 2]. Moreover, they help relating specific areas of the brain and functions they serve with the activated regions in the brain.

Modern structural and functional brain imaging methodologies proved a high level of anatomical and metabolic data that impact the diagnosis and management of epilepsy. Usually, the diagnosis of epileptic seizures is based on clinical history and physical evaluation. However, inadequate history and the presence or absence of a single symptom may lead to the misdiagnoses of this particular disorder. Thus, brain imaging provides supplementary evidence of the clinical suspicion. Besides the accurate assessment, these methodologies define the structural abnormalities that underlie seizure disorders. Moreover, patients who do not respond optimally to medical treatment might be candidates for epilepsy surgery. Therefore, brain imaging methodologies are essential to localize and lateralize epileptogenic areas accurately [3].

The Electroencephalography (EEG) source imaging technique has been developed as an identifier of the source of neuronal activity. It is a noninvasive technique that is used to measure electric potentials caused by any neural activity in the brain directly. Due to its high temporal resolution, low hardware costs, and direct measurements of electric potentials, EEG provides a complement (or a replacement) to other neuroimaging techniques, such as positron emission tomography (PET), single photon emission computed tomography (SPECT), and functional magnetic resonance imaging (fMRI). Furthermore, when it comes to investigating seizures, it is required to measure neuronal activity before, during, and after a seizure. Since it is possible to measure neuronal activity in real time using EEG, it is very useful in epilepsy diagnosis.

In order to perform EEG source localization, two problems should be solved: the forward and the inverse problems. In the forward problem, appropriate head models are used to obtain electric potentials on the scalp that are produced by neurons. Neurons on the other hand, are modeled as current dipoles. To solve this

problem, a mathematical model that approximates the primary current density of the source is developed. The approximated current density represents the brain activity to be localized by solving the inverse problem.

However, measuring signals on the surface of the scalp does not directly indicate the location of the activated neuron. This is because different source configurations may produce the same measured electric fields on the scalp. As a result, the only way to localize electric sources is by making prior assumptions on the generation of EEG signals. This is known as the inverse problem which involves locating the sources of neural activity. The inverse problem is then solved by implementing array processing based methods to reduce source localization error.

Array processing methods provide a potent signal processing tool for solving the inverse problem. Depending on the assumption made for sources that generate the electric fields, different algorithms can be utilized for source localization. A well-known source localization algorithm is the Low-Resolution Electromagnetic Tomography (LORETA) which is used to localize multiple distributed active sources. This algorithm assumes that neighboring neural populations are probable to undergo synchronous depolarization during evoked response or a discharge than the non-neighboring neurons. Another commonly used algorithm is the Source Affine Image Reconstruction (SAFFIRE). It is based on assuming that collected measurements via an array of sensors can be modeled as the superposition of independent contribution from distributed sources. A detailed discussion of different source localization methods, mathematical interpretation, and the advantages and limitation of each algorithm are presented in Chapter 3.

1.2 Motivation and Problem Statement

An epileptic seizure is defined as a temporary disruption of brain functions due to the hypersynchronous, the abnormal firing of cortical neurons. Epileptic seizures are sudden, transient, and usually brief. Approximately 1% of the population suffers from epilepsy, which makes it the second most common neurologic disorder after strokes [4]. Epilepsy is often controlled by a wide variety of medication. However, a number of patients will not respond optimally to medical treatment with either continued seizures or unacceptable side effects. As it is known, the temporal and frontal lobes are the usual locations of the epileptogenic zone. Thus, it is reasonable to assume that epilepsy treatment may affect the creative process since any mechanism

affecting chemical and structural connectivity in the brain has the potential to affect cognition, motivation, and talent. Some anti-seizure drugs lower arousal and motivation, making them counterproductive to the creative process [5].

Therefore, Surgery is recommended in these cases where the affected epileptogenic area is identified and surgically removed [3, 6]. Other surgeries that involve disconnecting pathways between parts of the brain are made to prevent the seizure from spreading to other parts of the brain [3]. Surgery outcomes are optimal when seizures are demonstrated to arise from one well-defined area that can be removed without functional compromise. Many imaging techniques have improved the pre-surgical structural analysis and surgery outcomes [3].

The grand challenge of this work is the accurate source localization of epileptogenic zones that need to be removed. Hence, the objectives of this thesis are to use the EEG source localization technique in order to determine epileptic sources with high temporal and spatial resolutions and to study the effect of reducing EEG sensors dimensionality in Source localization performance.

1.3 Research Methodology and Outline

In this report, the forward problem solution is obtained using two software packages called Advanced Source Analysis (ASA-lab) and Brainstorm. Boundary Element Method (BEM) is available in these softwares in order to model a realistic head using MRI image. Furthermore, the raw EEG data is a complex waveform that contains not only brain activity, but also random electromagnetic noise and unwanted electrical activities of nearby muscles (e.g. Heartbeats, eyeblinks, eye movement, etc.). Therefore, several pre-processing techniques are applied to the raw EEG in order to remove unwanted signals. Starting with removing and correcting artifacts, signals that have not originated from the brain are removed from the EEG data. Next, low-pass and high-pass filters are used to remove unwanted random noise frequencies. Recorded EEG signals of an evoked response (ERP) are analyzed using the ASA-lab software. Standard head model and MRI images are used to display potentials recorded by each electrode sensor and sources of the brain's neural activity. The head model, MRI image, and processed EEG signals are used for the purpose of localization.

Finally, Distributed sources based algorithm LORETA that can localize multiple simultaneously active sources, is investigated. This algorithm provides

smooth and better localization for deep sources with less localization error. At the end, LORETA is performed and the source of ERP signal is determined.

The rest of the thesis is organized as follows: Chapter 2 provides brief information about brain anatomy and neurons physiology, epilepsy as one of the major neurological disorders of the nervous system, and different imaging techniques used in the diagnosis of epilepsy. Chapter 3 outlines EEG source imaging (ESI) technique, its contribution in epilepsy diagnosis, and the steps towards solving the forward and inverse problems for accurate source localization. Moreover, it includes the literature review done on various existing dipole models and signal processing techniques used to solve the inverse problem. Three approaches for source modeling, which are the single, multiple, and distributed dipole models are introduced and prominent algorithms for each approach are reviewed. The advantages, drawbacks, and proposed enhancements of each of these models and signal processing techniques are also mentioned in this chapter. Chapter 4 includes EEG data processing and analysis procedure followed by LORETA localization results. Simulated and real epilepsy data source localization is performed using SAFFIRE and sLORETA methods in chapter 5. Furthermore, Epilepsy source localization using SAFFIRE algorithm is investigated on epilepsy clinical data and results are compared with medical reports in chapter 6. The effect of reducing the number of electrodes on localization performance is studied and future work is presented in chapters 7 and 8 respectively.

Chapter 2. Epilepsy Imaging Techniques

Epilepsy is a common disorder with recurrent and unprovoked seizures. Although symptoms of seizures may affect any part of the body, the electrical events that produce seizures occur in the brain. Evaluating patients with epilepsy depends on determining the seizure's type and causes. Number of steps is performed towards accurate diagnosis of epilepsy such as medical history, blood tests, and brain imaging. Brain imaging is an important part of the diagnostic process not only to confirm a diagnosis of epilepsy, but also to determine epileptogenic regions.

In this chapter, anatomy and physiology of the human brain is provided along with information on epilepsy as well as different brain imaging techniques that are used in epilepsy diagnosis.

2.1 Brain Anatomy

The brain is considered as the main and the most complex part of human body. It consists of three main parts which are the cerebrum, cerebellum, and the brain stem as shown in Figure 2-1. These parts work together to control every action in our daily life. However, each part has its own function. The cerebrum or cortex is associated with thought and action functions, and it is split into four sections called lobes. The cerebellum, which is similar to the cerebrum, is associated with movement coordination, posture, and balance regulation. The brain stem is responsible for vital life functions such as breathing, blood pressure, heartbeat, hormone secretion, etc.

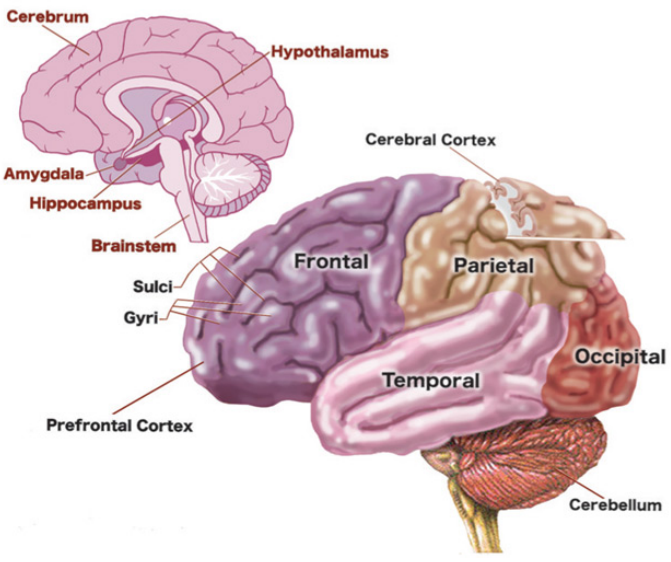

Figure 2-1 Brain components [7].

In the early history of neuroscience, observing the brain meant visually examining its anatomy, which involves the convolutions of the cerebral hemisphere, the nerve fibers, gray matter regions, and neurons structure. However, in the later twentieth century, electrical activity of neural tissue began to appear, and the nature of propagated signal began to reveal [8]. Electrical currents flowing in the brain's neurons are produced and cause electric and magnetic fields inside the brain. Neurons affect and are affected by other neurons through communication using chemical and electrical signals. Neurons comprise of dendrites, cell body (soma), axon and the myelin [9]. In simple words, the dendrites collect information from other neurons, then the information is received by the cell body which produces an electric signal that is called the *action potential*. The action potential propagates in the axon. Then, chemical signals are released into the synaptic cleft. These signals are called neurotransmitters, which latch onto the receptors of the target neuron. The received signal may cause an increase or decrease of the membrane potential of the target neuron.

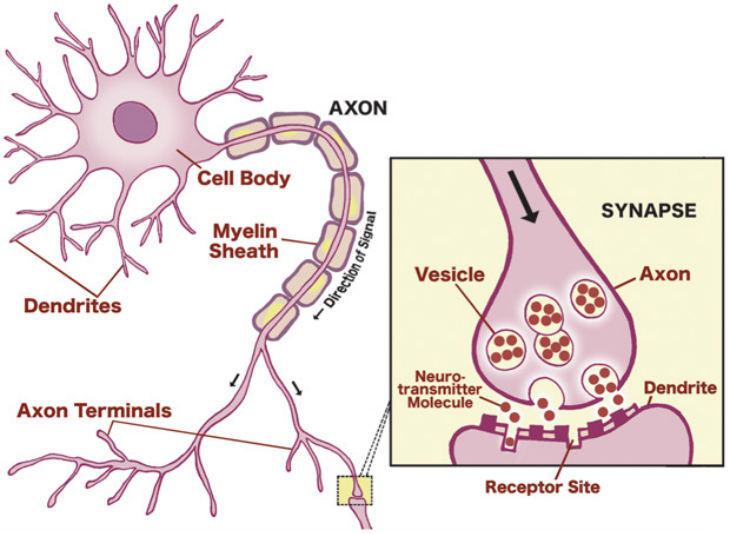

Figure 2-2 Communication between neurons [7].

Most of the major discoveries regarding the nature of neural activity were obtained with electrophysiological recordings of neurons. These recordings allow direct observation of electrical currents and potentials generated by single nerve cells with high spatial and temporal resolution [8]. Different techniques and imaging methods can be used for recording neural activity such as electroencephalography (EEG), magnetoencephalography (MEG), functional magnetic resonance imaging (fMRI), and Positron emission tomography (PET).

Structural, biochemical, or electrical abnormalities in the brain or other nerves can cause a neurological disorder of the nerves system. There are many recognized neurological disorders. Epilepsy is considered as the most common serious neurological disorder in the world [10].

2.2 Epilepsy

Epilepsy is the condition of recurrent, usually unprovoked seizures, it cannot be considered a single disease but rather an extensive collection of conditions with a range of underlying etiologies and pathologies sharing the fundamental characteristics of these recurrent seizures [10].

Diagnosis of epilepsy depends on the correct classification of epileptic seizures and epilepsy syndromes. A wide range of conditions must be considered in the diagnosis process since the misidentification of non-epileptic conditions as epilepsy may lead to unnecessary treatments that are for sure may be harmful and can delay the start of appropriate therapy. The first step in epilepsy diagnosis is essentially clinical evaluation, which is based on the detailed description of the events experienced by the patient before, during and after a seizure. In addition to patient medical and social history, routine blood tests should be performed to detect cardiac arrhythmias and conduction abnormalities.

2.3 Imaging Techniques for Epilepsy Diagnosis

Many investigational technologies are used to support the clinical diagnosis of epilepsy and help with the classification of seizures [10]. Brain imaging is one of the basic steps towards accurate clinical evaluation and diagnostic. It can be divided into structural and functional imaging. Structural imaging of the brain looks for underlying structural abnormalities, while functional imaging identifies focal abnormalities in cerebral physiology. In spite of the fact that functional imaging has a limited role in epilepsy diagnosis, it is considered to be very useful in the workup for epilepsy surgery.

2.3.1 Structural Imaging

Magnetic Resonance Imaging. It is considered to be the modal of choice in the surgical planning and postoperative follow up drug-resistant focal epilepsy which consist are 20 to 30% of epilepsy cases [11]. The choice of MRI is because of its high sensitivity and specificity in comparison with Computed Tomography (CT) for

identifying structural lesions. Once, CT accepted as the first imaging modality to be performed, but now it is considered supplementary in the detection of calcification as in the case of epileptogenic tumors. However, CT should be performed if MRI is unavailable and in patients with cardiac pacemakers or severe claustrophobia that result a contraindicated MRI.

The principle role of MRI is to define structural abnormalities that may be a cause of disorders like epilepsy. *Figure 2-3* shows multiple gray matter heterotopia which may cause recurring seizers.

There are number of factors affect the success of MRI in detecting abnormalities, they can be determined by the scanner and applied techniques, the experience of the radiologist and, of course, the nature of epileptogenic lesions [12]. Computational post-processing of structural MRI techniques is used to quantify brain morphological features and allow the use of statistical inferences instead of visual inspection to identify abnormalities.

The first goal of MRI in epilepsy patients is the detection of epileptogenic regions. With careful MRI reading, lesions are visible without additional contrast medium injections which are usually needed to characterize a lesion but not to find it [13]. A number of epilepsy-relevant features that can be measured with brain MRI scan are local gray matter volume, cortical thickness, sulcus depth, blurring of the boundary between gray and white matter in the cortex and more exotic measures that quantify local spatial properties of tissues such as cortical gyrification and texture analysis.

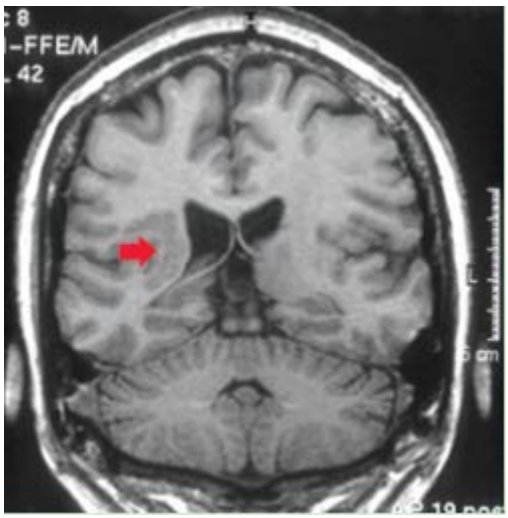

Figure 2-3 MRI scan shows multiple gray matter heterotopia [10].

Increasing spatial resolution requires a development of better hardware, the most standard methods is the use of higher field MRI scanners. However, there is still limited evidence that the use of this imaging technique is useful for imaging nonlesional epilepsy cases which is due to the limited availability high-field scanners, appropriate acquisition sequences and lack of systematic studies [14]. In children with EEG findings pointing to a genetic epilepsy syndrome, the use of MRI is typically unrevealing. Because some non-genetic epilepsies may sometimes resemble these genetic epilepsy syndromes, MRI is recommended in these patients if they present with any atypical features such as abnormal neurologic or intellectual development, difficult-to-treat seizures, or unusual course. Also, for children with focal, possibly drug-resistant epilepsy syndromes, the effort to generate high-quality MRI is greatest. Because these patients may be uncooperative and unable to tolerate sequences lasting around 5 min, hence, anesthesia including sedation and intubation is needed [15].

Functional Magnetic Resonance Imaging. Because of the lack of ionizing radiation in MRI scanners, functional MRI has come out as one of the popular means of visualizing brain activity. Its primary use has been in localizing activation in response to sensorimotor or cognitive tasks. And since epilepsy is a functional disorder that –in many cases- may not be accompanied with outrageous abnormalities in structural imaging, fMRI has received attention and used to examine regional changes in brain functions that are associated with ictal or interictal states. Furthermore, fMRI has been used as a part of preoperative evaluation for epilepsy surgery to assess localization of language, memory, and other functions. It is simply MRI scanning with blood flow and/or metabolism attribution in significant tissue contrast. The changes are on the order of precent or less of the overall signal intensity, however, modern MRI scanners are stable to measure such small changes in a reliable way [16].

Patients are instructed to perform specific tasks following a strict protocol, the intracerebral localization of the tested function is determined via a surrogate parameter (spatial distribution of activation-related cerebral perfusion changes). As a response to the task execution, neural activity and oxygen consumption are elevated in areas associated with the performed task. There are two main reasons to perform fMRI studies in epilepsy patients, first, it is used to evaluate the relationship of a lesion with eloquent cortex. And the second reason is to assess hemispheric dominance.

Mainly there are two primary contrast mechanisms used for fMRI which are blood oxygen level dependent (BOLD) contrast and perfusion contrast. BOLD contrast reflects a complex interaction between blood flow, blood volume and hemoglobin oxygenation [17]. While perfusion contrast is obtained using arterial spin labeling which uses magnetically labeled arterial blood water as flow tracer. Figure 2-4 shows BOLD contrast as a response to inter-ictal epileptic activity. BOLD contrast mechanism has been raised as the method of choice for imaging brain activity using fMRI because it is easy to obtain and provides higher signal-to-noise ratio for task-specific activation.

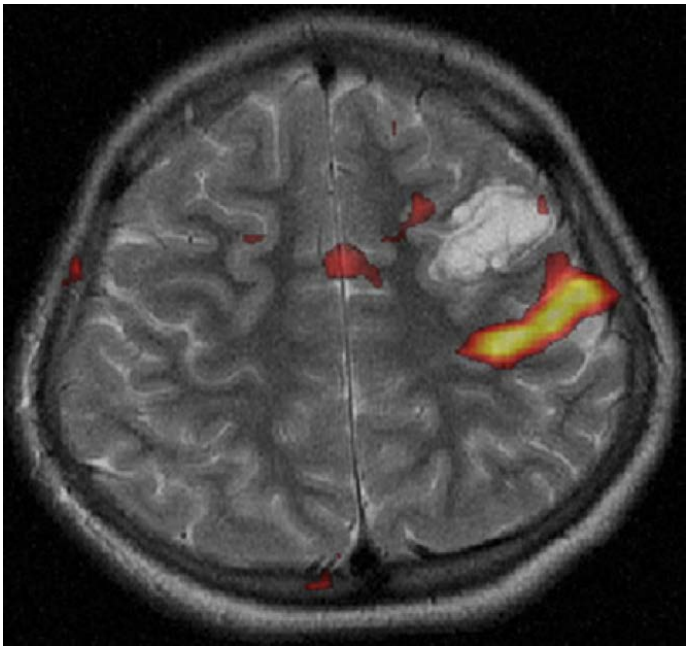

Figure 2-4 fMRI shows BOLD activation on one gyrus beyond the right frontal [17].

All fMRI studies use time-series data acquired by using snapshot imaging method, where the entire brain volume is sampled every 1-3 s. This method places high demands on hardware performance and data processing speed. Most of them have used multiple blocked-trial designs with alternating epochs of task and control conditions. Sensitivity is maximized through this approach because large signal changes are sustained [16].

Recently, the spread of high field scanners with high-performance gradient systems have provided high sensitive fMRI which improved the quality and reliability of fMRI results. BOLD fMRI methods can be used to localize seizure foci during

clinical or subclinical seizures as in [18, 19], where reports showed transit focal activation that correlated with clinically determined seizure foci.

When compared to EEG spatial resolution property, fMRI has an excellent spatial resolution and allows the localization of brain regions by taking advantage of the change of neuronal activity during an experimental perturbation compared to control conditions. This change is combined with a modification of the ratio of the concentration of oxy and de-oxy hemoglobin in the blood that is measured through the BOLD effect. In contrast to EEG, fMRI has a poor temporal resolution, the measures of neuronal currents on the order of seconds not milliseconds.

Hence, EEG-fMRI combined recording exploit the complementary features of the two techniques to overcome the limitations of each. But it is extremely challenging to record EEG signals during fMRI scanning because of the large currents induced in electrodes due to the magnetic field-gradient pulsation required for MRI. On the other hand, electrodes can serve as a conduit for radio frequency noise that may degrade MRI data. To overcome these challenges several methods have evolved over the past years. As in [20], EEG-triggered fMRI is used to localize changes in regional brain activity associated with paroxysmal electrographic activity but it did not obtain these modalities simultaneously. Furthermore, as in [21-23], high-resolution digitization and post-processing strategies are used to allow the intense and reproducible gradient artifacts to be eliminated, providing interpretable EEG data during scanning. As a result, this allowed the fMRI correlates of spike foci and other paroxysmal events to be even more convincingly demonstrated as in [24-26].

In many cases of drug-resistant focal seizures, standard magnetic resonance imaging (MRI) scans on patients for pre-surgical evaluation- fail to visualize a clear epileptic seizure source, thus an introductory noninvasive EEG analysis is required. Combined EEG and fMRI records are considered to be a less invasive alternative since they provide high spatial and temporal resolution of brain regions generating inter-ictal epileptiform activity [27].

In the general fMRI study involving sensory, motor and cognitive functions, experimental and control conditions are identified based on the task. In epilepsy studies, the control conditions occur when the EEG is at the baseline and the experimental condition corresponds to the presence of epileptic discharge [28].

2.3.2 Functional Imaging

The main technologies which are used for functional imaging are single photon emission computed tomography (SPECT) and positron emission tomography (PET). As mentioned before, these functional imaging modalities have a role in the pre-surgical evaluation of epilepsies as they are able to detect epileptogenic foci in morphologically unnoticeable areas. In addition, they provide a better understanding of the neurobiology of epilepsy.

Single photon emission computed tomography. According to the fact that SPECT demonstrates the functional activity through measuring blood flow inside the brain, it is considered to be valuable for diagnosis and localizing several neurological disorders including epilepsy [29]. Its application in epilepsy is based on the assumption that the increased ictal neuronal activity occurring during epileptic seizures is associated with an increase in metabolism and regional cerebral blood flow (rCBF) [30].

Figure 2-5 shows a SPECT images for a patient with right hippocampal epilepsy.

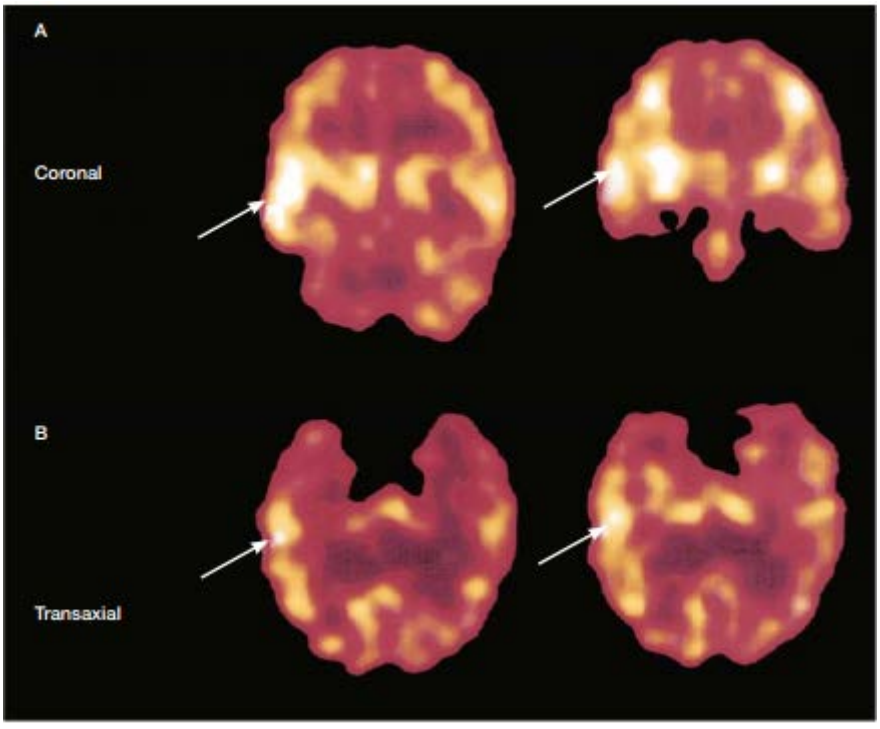

Figure 2-5 Ictal SPECT shows increased perfusion in the right temporal lobe [3].

Iodine-123 and technetium-99-m-labeled radiopharmaceutical are commercially available and used as a tracer for brain perfusion SPECT. Their small

molecular size and lipophilicity cause the ability to cross the intact blood-brain barrier rapidly and to be distributed proportionally to the blood flow in cerebral tissue, then to remain in the brain for a sufficient time (greater than 30 minutes) to permit image acquisition [31]. ^{123}I-labeled amines were initially used but it was found that these tracers reach peak brain activity after injection by 20 minutes and show redistribution over time, which results in reuptake into the cerebral cortex that is not proportional to rCBF. To overcome this problem ^{99m}Tc-hexamethylpropyleneamine-oxime (^{99m}Tc-HMPAO) and ^{99m}Tc-ethyl cysteinate dimer (^{99m}Tc-ECD) are used for investigating rCBF and they are considered to be the most frequently used tracers. In comparison with ^{123}I-labeled, they have a quicker initial uptake in brain and reach the peak within 2 minutes of injection without redistribution. Hence the initial tracer uptake and distributed correspond to rCBF at the time of injection and remains unchanged up to at least 2 hours independent of rCBF variation occurring after fixation time. Therefore, after injecting the radiotracer into the patient, rCBF images reflecting the distribution at the moment of seizure occurrence can be acquired later with SPECT camera after the recovery from the seizure. This technique rendered to be useful and affordable for clinical routines because of the appropriate hold-time of technetium, which is 6 hours, and the stability of the tracer [30].

Many researchers have agreed that epileptic foci are localized in a reliable manner with a subtraction SPECT image. This image is created via the information from individual studies, interictal SPECT and ictal SPECT. Where interictal SPECT study illustrates the brain when it is not undergoing an epileptic seizure and the ictal illustrates the brain during the epileptic event. As stated in [32] Ictal SPECT has shown to be more accurate for localization of temporal lobe seizures when the radiotracer is injected immediately after the seizer. However, the injection of the tracer is performed after the seizure start and takes time before it gets to the brain, this delay should be overcome. Therefore, the increased in rCBF showed by ictal SPECT that is related to seizure might also indicate propagation from the area of ictal onset. Moreover, when the delay between seizure onset and tracer application is too long, false localization of the ictal seizure can be observed. This phenomenon is called “postictal switch” [33].

Several studies have demonstrated that ictal SPECT has better quality when compared to interictal SPECT in identifying the location or the lateralization of epileptic seizures of a patient with temporal lobe epilepsy (TLE). [34-37] indicated a

sensitivity between 73 and 97% for ictal SPECT and only 50% for interictal SPECT. As cited by medical experts in [38], probable epileptic foci often display behaviors between and during epileptic events regarding blood flow in the tissues.

Although SPECT image subtraction is effective at demonstrating changes in perfusion between studies, there are some constraints in its utility. Many interactive processing steps are required to obtain subtracted SPECT images which require input from users familiar with brain dynamics. Also, Programming tools used for SPECT image analysis are not fully automated. Another limitation and the most important one is that the image obtained through SPECT subtraction does not always depict a localized epileptic focus localization.

A factor that limits the quality of the reconstructed image is the tissue attenuated due to the nonlinear relation between the ray sums of activity in the patient and the gamma ray emissions collected by the SPECT system. In addition to that, spatial resolution, scattered radiation, and image noise affect the quality and accuracy of the acquired image projections [39].

To overcome these limits better instrumentation or better correction algorithms are required. Authors of [40] have made a contribution to the automation of the processing and interpretation of SPECT images. It was determined that for the ten sets of patient SPECT image data, the automated SPECT image analysis algorithm obtained 91.3% average rate of accuracy for epileptic focus. Since the projection information required for SPECT is acquired by gamma ray detector, the quality of the projection will depend on the accuracy of the detector. Hence the detectors should be of good energy resolution, good spatial resolution.

In spite that SPECT continues to progress with major improvements in instrumentation and reconstruction, the limits of spatial resolution and sensitivity have not yet been reached for clinical devices [39].

Positron Emission Tomography. PET is considered to be an important tool for identifying the ictal zone and understanding neurobiology and functional alteration associated with different types of epilepsy. Many PET studies, such as measurements of glucose, serotonin and oxygen metabolism, cerebral blood flow and receptor bindings are available for epilepsy. 18Fluoro-2-deoxyglucose (18F-FDG) PET imaging of the brain is a prominent and widely available technique. It allows quantification of cerebral glucose metabolism and it’s an indirect marker of neuronal

activity. Epileptogenic regions can be detected as interictal hypometabolic regions as in Figure 2-6.

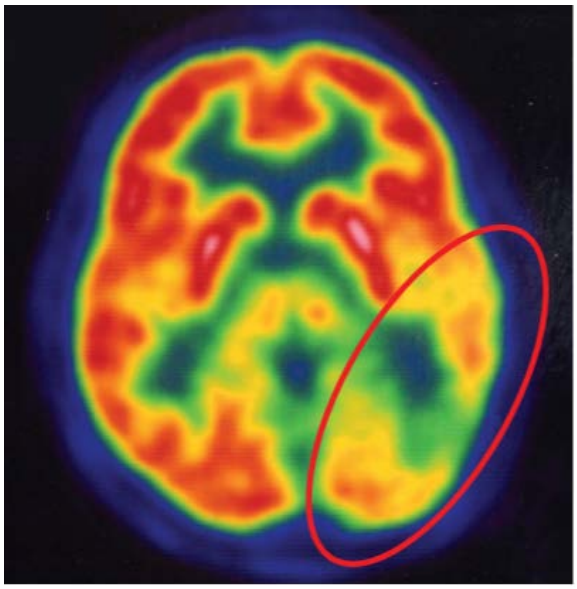

Figure 2-6 PET shows interictal hypo metabolism over the left temporal and occipital areas [10].

FDG PET is the most commonly utilized technique in routine clinical practice. In comparison with SPECT studies, researches have demonstrated that the sensitivity of interictal FDG-PET is higher than interictal SPECT. And for the lateralization and localization of epileptogenic foci, FGE-PET is similar to ictal SPECT in pre-surgical patients' who have noncontributory EEG and MRI. In addition, FDG-PET provides additional important information on the functional status of the rest of the brain [41]. Interictal FDG PET can also be of some value when there is possibly more than one focal ictal zone or when clinical data are discordant with EEG findings. FDG PET yield can be improved by using statistical analysis methods, such as statistical parametric mapping (SPM) as well as by PET/MRI co-registration on a clinical level which improves sensitivity [2].

However, the main limitation of interictal FDG-PET is that it cannot define the surgical margin exactly as the area of hypometabolism usually extends beyond the epileptogenic zone.

It is important for the spread of epileptic activity to quantify the specific ligand-receptor relationships which are allowed by PET. Several PET receptors ligands have been used in epilepsy diagnosis to investigate its neurochemical basis [30]. PET receptor imaging technique have partially entered clinical routine and it can

be used to investigate new treatment approaches. However, it is performed in limited centers and requires well-experienced staff as well as on-site equipment. On the other hand, practical limitations of using any of these radiotracers include the lack of commercially available radiotracers, short half-life that necessitates an onsite cyclotron, moderate signal-to-noise ratio, and the need for arterial blood sampling to model tracer-binding features. In addition, to date, none has demonstrated a clear clinical role in nonlesional epilepsy [41].

Electroencephalography. Electroencephalography recording is used to measure the difference in potentials between two electrodes placed in an array across the scalp. It carries high specificity for epilepsy for which the cardinal symptoms are hard to be mistaken for others and are rarely seen in conditions outside epilepsy as noticed in Figure 2-7. However, its ability to confirm epilepsy in patients who have it is considered to be limited. Therefore many techniques have been arisen for EEG to help elicit epileptic abnormalities and hence helping clinicians in the diagnosis of epilepsy [4]. More detail about EEG and its uses in epilepsy source localization will be discussed next chapter.

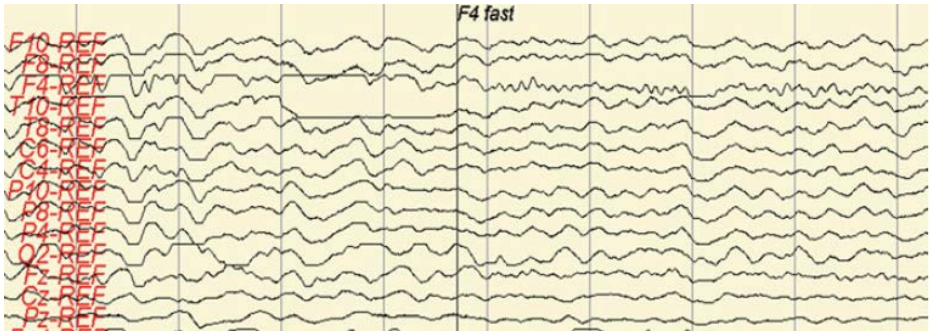

Figure 2-7 EEG recording shows seizure onset from the right frontal region (F4) [6].

Magnetoencephalography. Magnetoencephalography (MEG) where magnetic field associated with intracellular current flows within neurons are measured between seizures. It is usually used for patients with normal neuroimaging results. When combining MEG with structural imaging (MRI) it is known as magnetic source imaging (MSI) which considered to be one of the noninvasive tools for epilepsy localization [42].

Since MEG measures extracranial magnetic fields perpendicular to the direction of intracellular electrical currents in active cortical neurons, it is sensitive to currents flowing tangential to the scalp which is corresponding to sulcal activation. Based on the fact that magnetic field measured by MEG is less affected by

intervening tissue layers, MEG is a useful clinically usable tool in pre-surgical localization of epileptogenic foci and allows reliable localization of brain activity [43] as shown in *Figure 2-8*. In addition, MEG can be estimated using simple spherical head model since it is less susceptible to the irregularities of head geometry. The systematic review done in [43] has shown that the sensitivity and/or specificity of MEG as a primary diagnostic tool has not been consistently high and the effectiveness of MEG in impacting epilepsy surgery outcome is still lacking.

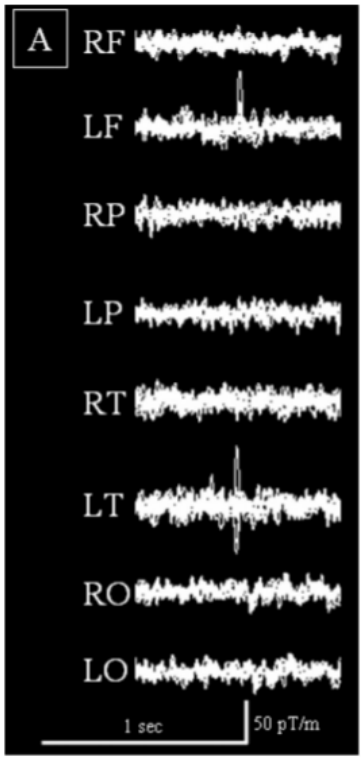

Figure 2-8 MEG signal shows left fronto-temporal interictal spikes [44].

There are two approaches used to confirm the accuracy and clinical validity of MEG in the localization of epilepsy, which are the direct and indirect approaches. Direct approaches reflect work done with implanted dipoles using special intracranial IC electrodes or simultaneous EEG and MEG recording. Whereas indirect methods come from studies that demonstrate colocalization with epileptogenic regions that are visible or confirmed through structural or functional imaging, subsequent intracranial EEG and successful surgical outcomes [45].

As mentioned previously, investigating epileptic syndromes determining whether it is epileptic seizure or not requires many steps toward accurate diagnosis and localization of epileptic area. The imaging capabilities provided through the integration of SPECT, PET, MRI, EEG, and MEG are often used. This multimodality

imaging which combines structural and functional information helps in improving the ability to detect and define epileptogenic lesions. The most sensitive methods for identifying relevant epilepsy-related brain regions will likely involve a combination of the above-mentioned features [14].

Chapter 3. EEG Source Imaging In Epilepsy

3.1 EEG Source Imaging Technique

As we mentioned before, EEG is a functional brain imaging technique that records the brain's electrical activity. Electrodes are placed in contact with the scalp at selected locations above cortical regions. EEG measures the potential difference between pairs of electrodes. EEG has many clinical uses and it is considered an important tool to measure neural activity and identify the area of cortex that is responsible for generating spikes and epileptic seizures.

Usually, to identify the type of epilepsy, a clinician relies on simple visual analysis of EEG recordings. However, when it comes to epilepsy surgery evaluation, computational techniques are used to more precisely identify the cortical locations that cause abnormal seizures. Therefore, EEG source imaging (ESI) technique have been developed as an identifier of the source of evoked potentials.

In routine EEGs, more than 50% of patients with epilepsy will have a normal trace. However, with repeated recordings, epilepsy can be better diagnosed. It is preferable to detect interictal and ictal events in case of negative routine EEG using portable equipment to allow prolonged recording in the patient's usual environment. Moreover, it is possible to achieve behavioral correlation in patients by video monitoring during the EEG. Video monitoring is considered to be an integral part of the evaluation of epilepsy and may be the only way to distinguish epileptic from non-epileptic seizures.

Recent technology developments have allowed simultaneous EEG recordings with fMRI so that interictal EEG changes can be spatially localized to provide better understanding of the spatiotemporal mechanism of the generation of epileptiform activity in the brain.

The development of mathematical techniques is required for EEG measurements analysis in order to understand the spatiotemporal activities in the brain. However, it is impossible to determine the exact location of an electrical source in the brain from only recorded EEG data. To overcome this, the characteristics of the head and internal structure and the location of sources should be modeled to predict the scalp voltage field. This operation is so called the forward problem. After solving the forward problem, it becomes possible to estimate current sources from which neural activity originate by solving the inverse problem.

3.2 Forward Problem

The forward problem for EEG is complicated by the difficulty of predicting the surface field for a given source within the head structures. To solve this problem, a set of known conditions for the head model is specified and then the potential at the recording electrodes is calculated. Generally, for a specified source, only one field potential is possible on the surface of the head, which results a unique forward solution [46]. To offer the best forward solution, a realistic head model can be achieved using an individual's MRI.

Mathematically, the forward problem can be modeled as, [47]

$$V_{ij} = \int L_{ij}^{M}(r) \,.\, J^{p}(r)\, dV \tag{1}$$

where V_{ij} denotes the potential difference measured between electrode *i* and *j*. L_{ij}^{M} is the leadfield for electrode pairs *i* and *j* and is expressed in Ω/m. It depends on the location configuration of the electrodes. $J^{p}(r)$ represents the primary current density produced by a source in location r. As long as the approximated leadfields and primary current densities are known, a unique solution for the electric potential can be obtained. Hence, the forward problem is considered to be well posed.

3.2.1 Quasi-static Approximation of Maxwell's Equations

Since the useful frequency spectrum for EEG signal is found to be below 1 KHz, quasi-static approximation can be applied to Maxwell equations by eliminating the terms with time dependency. Therefore, Maxwell equations for electric and magnetic fields *E* and *H* respectively can be written as:

$$\nabla \times \boldsymbol{E} = 0 \tag{2}$$

$$\nabla \times \boldsymbol{H} = \boldsymbol{J} \tag{3}$$

Where $\boldsymbol{E}$ is the electric field intensity (V/m), $\boldsymbol{H}$ is the magnetic field intensity (H/m) and $\boldsymbol{J}$ is the current density (A/m^2).

By taking divergence of both sides of (3) the resulted equation is,

$$\nabla.(\nabla \times \boldsymbol{H}) = \nabla.\boldsymbol{J} \tag{4}$$

Applying the identity $\nabla.(\nabla \times \boldsymbol{F}) = 0$, the left-hand side of (4) will be,

$$\nabla.\boldsymbol{J} = 0 \tag{5}$$

The total current density produced by neural activity in the brain is the sum of primary current density $\boldsymbol{J_p}$ generated by neural activity and secondary currents densities $\boldsymbol{J}_\Omega$ that flow passively in the conductive medium as in (6).

$$\mathbf{J} = \boldsymbol{J_p} + \boldsymbol{J}_\Omega \tag{6}$$

As stated before, the source of brain activity is characterized by the primary current density $\boldsymbol{J_p}$. Nevertheless, localization accuracy is improved by modeling the volume currents.

3.2.2 Current Dipole as a Source

An excitatory postsynaptic potential may be induced when the axon of a presynaptic neuron synapse with basal dendrites of a postsynaptic pyramidal neuron. The postsynaptic potential can be represented by a current dipole. However, the dipole model is valid when assuming that neuronal activity is dominant in a small brain area.

For a small region of activated cortex, current dipole $\boldsymbol{Q}$ at $\boldsymbol{r_Q}$ can be considered as a concentration of the primary current density $\boldsymbol{J_p}$ to a single point[47]:

$$\boldsymbol{J_p}(\boldsymbol{r}) = \boldsymbol{Q}\,\delta(\boldsymbol{r} - \boldsymbol{r_Q}) \tag{7}$$

where $\delta(r)$ is the Dirac delta function. As mentioned, the forward problem involves calculating scalp potential (V) from a given current distribution within the brain. Therefore, $\boldsymbol{E}$ can be represented to satisfy equation (2) as follows

$$\boldsymbol{E} = -\nabla V \tag{8}$$

Based on the constitutive relations between the electric field quantities,

$$\boldsymbol{D} = \epsilon \boldsymbol{E} \tag{9}$$

$$\boldsymbol{J} = \sigma \boldsymbol{E} \tag{10}$$

where the ϵ and σ are the permittivity (F/m) and conductivity (S/m) of the medium respectively. The volume secondary current density is represented as,

$$\boldsymbol{J}_\Omega = \sigma \boldsymbol{E} \tag{11}$$

$$\boldsymbol{J}_\Omega = -\sigma \nabla V \tag{12}$$

From (6) we obtain,

$$\mathbf{J} = \boldsymbol{J_p} - \sigma \nabla V \tag{13}$$

As we before stated in equation (5) and by applying divergence on both sides of equation (13)

$$\nabla . \boldsymbol{J_p} = \nabla . (\sigma \nabla V) \tag{14}$$

Equation (14) can be solved for V either numerically implementation of finite element techniques, or analytically by using appropriate boundary conditions [47].

3.2.3 Head Models

To solve the inverse problem, an accurate head model is required. It basically determines the way sources are located in the brain. It includes the geometrical and electromagnetic properties of the volume and can be mathematically expressed in the leadfield matrix. The leadfield matrix (or Gain matrix) resulted from solving the forward problem represents the linear relation between the sources and measurements. *Single Sphere Head Model.* This head model is the simplest and often used head model [48]. It assumes uniform conductivity and its analytical solution is easy and fast to calculate. However, in reality, the head is inhomogeneous and the uniform conductivity assumption does not suffice. Also, source localization accuracy is found to be limited and insufficient when considering certain regions of the brain like the frontal and frontal-temporal regions [49].

Multiple Spheres Head Model. Multiple spheres model consists of three layers with different conductivities. Each layer is assumed to be concentric, homogenous spherical shell to represent head compartments (scalp, skull, and brain). This Model is used in the most clinical and research applications related to EEG source localization.

Realistic Head Model. Anisotropic, inhomogeneous and non-spherical heads can be obtained using realistic volume conductor model. The lead-field matrix is accurate and results in high localization accuracy. The most common modeling techniques used for realistic head modeling are Boundary Element Method (BEM) and Finite Element Method (FEM).

BEM assumes homogeneity and isotropy within each region of the head. Whereas FEM takes into account the individual anisotropic conductivities for each element. FEM head model is shown in Figure 3-1.

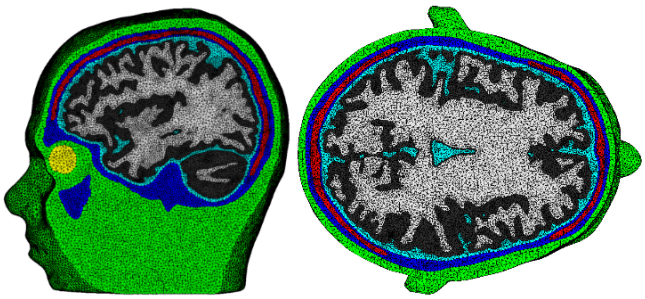

Figure 3-1 Realistic head model using FEM.

3.3 Inverse Problem

The inverse problem of EEG involves locating the sources of the primary current densities $J^p(r)$ and it requires a set of measured potentials and approximated lead-field obtained by solving the forward problems. Hence, modeling the forward problem with *priori* assumptions of the source and head structure is required to solve the inverse problem. These assumptions can substantially influence the outcome of source localization using ESI, and they are considered important in determining whether the solutions can only explain the data or it can provide neurophysiological information regarding the source [46]. Various signal processing based techniques are used to solve this problem and estimate source locations and amplitudes.

3.4 Brain Source Models

As mentioned earlier, neuronal activity source is modeled as a dipole. Three approaches are stated in the literature and will be discussed along with the common source localization algorithms in the following subsections.

3.4.1 Single Source Dipole Model

The single equivalent current dipole is the most commonly used source model in the clinical setting. It is based on the assumption that at any given time instant, the detected potential represents activity from a single, infinitely small cortex area [46]. Hence, the dipole model will never reflect biological fact and reality will be approximated in a limited number of conditions, such as epileptic spikes or the early component of the auditory evoked potential [46].

The most common algorithm for this model is the Least Squares source estimation (LS) where six parameters are assigned to each dipole: one parameter for the magnitude, three location parameters (x, y, z) and two orientation parameters (azimuth and elevation). This algorithm works as follows: First, the number of dipoles and their initial locations are selected. Second, the electric potential is computed for

the provided dipole parameters, i.e. solving the forward problem. After that, the computed electric potential is compared with the actual electric potential and the squared error is calculated. The measure of fit in the LS is defined by Frobenius norm as in equation (15) [2]. An iterative non-linear search algorithm is applied to minimize the squared error over all dipole parameters until some minimization criteria are met.

$$F_{LS}(\{r, \Theta_i\}, S) = \|\boldsymbol{V} - \boldsymbol{K}(\{\boldsymbol{r}, \boldsymbol{\Theta}_i\})\boldsymbol{J}^T\|^2 \quad (15)$$

where $\boldsymbol{V}$ is the measured potential and $\boldsymbol{K}(\{\boldsymbol{r}, \boldsymbol{\Theta}_i\})$ is the gain matrix (leadfield matrix) that relates a set of dipoles to a set of locations, where $\boldsymbol{r}$ is the three location parameters and $\boldsymbol{\Theta}_i$ is the two orientation parameters. $\boldsymbol{J}$ is the generalized matrix of sources amplitudes.

There are three mostly used dipole models: the fixed dipole model, the moving dipole model, and the rotating dipole model. These dipole models are used with most EEG clinical and experimental data [2]. The Least-square approach (LS) can be applied to these models. In the fixed dipole model, the dipole magnitude is estimated assuming constant location and orientation within a given interval. On the other hand, the moving dipole model results when the dipole location is not fixed, hence, LS model is applied to each time interval for varying dipole parameters. In the rotating dipole model, orientations and magnitudes of the dipole are allowed to vary, but, the location of the dipole is constrained to one point.

The least-square model has a number of drawbacks. The main one is that the number of dipole sources must be determined by the user before applying the algorithm. Moreover, as the number of dipole sources increases, the least-square cost function becomes nonconvex which results in local minima.

3.4.2 Multiple Sources Dipole Model

In this model, it is assumed that the recorded voltage field using EEG can represent activities from more than one source. Hence, a more advanced dipole model, such as the spatiotemporal multiple source model, is applied. In this technique, the entire block of data is used to calculate the least square fit under the assumption of fixed locations and orientations of numerous dipoles over a given time interval. The multiple dipole model goal is to identify the lowest number of dipoles that can explain the measured scalp potential over time. Moreover, the correct estimation of the number of sources is a critical issue for multiple dipole models.

Many techniques have been developed and are able to scan brain sources without *a priori* knowledge of the optimal number of dipoles over a given data period. Multiple signal classification (MUSIC) is a technique for localizing multiple sources. It can provide computational advantages over LS methods. In addition, it allows complete searches over space parameter of each source that results in avoiding problems with local minima experienced in searching for multiple sources over a nonconvex surface [50]. In this technique, data covariance matrix is decomposed into signal and noise subspace using Eigen decomposition. It is performed under the assumption that sources are located at a position where the dipole forward solution is orthogonal to noise subspace [2]. The received data vector is a linear combination of the leadfield matrix through,

$$\boldsymbol{y}(\mathrm{n}) = \boldsymbol{S}\boldsymbol{x}(n) + \boldsymbol{v}(n) \tag{16}$$

Where $\boldsymbol{S}$ is a normalized leadfield matrix, $\boldsymbol{x}(n)$ is a source vector and $\boldsymbol{v}(n)$ is a zero-mean additive White Gaussian noise vector. The spatial covariance matrix is computed by assuming uncorrelation between the signal vector $\boldsymbol{x}(n)$ and the noise vector $\boldsymbol{v}(n)$. The spatial covariance of the observation is represented as,

$$\boldsymbol{R} = E\,[\,\boldsymbol{y}(n)\boldsymbol{y}(n)^H] = E\,[\,\big(\boldsymbol{S}\boldsymbol{x}(n) + \boldsymbol{v}(n)\big)\,\big(\boldsymbol{S}\boldsymbol{x}(n) + \boldsymbol{v}(n)\big)^H\,] \tag{17}$$

$$\boldsymbol{R} = \boldsymbol{S}\,E[\boldsymbol{x}(n)\boldsymbol{x}(n)^{\boldsymbol{H}}]\boldsymbol{S}^{\boldsymbol{H}} + E[\boldsymbol{v}(n)\boldsymbol{v}(n)^{\boldsymbol{H}}] \tag{18}$$

$$\boldsymbol{R} = \boldsymbol{S}\,\boldsymbol{R}_{\boldsymbol{xx}}\boldsymbol{S}^{\boldsymbol{H}} + \sigma^2\boldsymbol{I} \tag{19}$$

where E is the statistical expectation, $\boldsymbol{R}_{\boldsymbol{xx}}$ and $\sigma^2\boldsymbol{I}$ are the source and noise correlation matrices, respectively. Furthermore, the eigen decomposition of $\boldsymbol{R}$ is represented as,

$$\boldsymbol{R} = \boldsymbol{E}_{\boldsymbol{S}}\,\boldsymbol{\Lambda}_{\boldsymbol{S}}\boldsymbol{E}_{\boldsymbol{S}}^{\boldsymbol{H}} + \sigma^2\boldsymbol{E}_{\boldsymbol{N}}\,\boldsymbol{E}_{\boldsymbol{N}}^{\boldsymbol{H}} \tag{20}$$

where $\boldsymbol{E}_{\boldsymbol{S}}$ and $\boldsymbol{E}_{\boldsymbol{N}}$ denote the signal and noise subspace and $\boldsymbol{\Lambda}_{\boldsymbol{S}}$ represents the diagonal matrix of the signal that contains eigenvalues that corresponds to the signal subspace.

MUSIC algorithm searches for the deepest local minima of,

$$\eta_{MUSIC} = \boldsymbol{s}_{\boldsymbol{k}}^{\boldsymbol{T}}\widehat{\boldsymbol{E}}_{\boldsymbol{N}}\widehat{\boldsymbol{E}}_{\boldsymbol{N}}^{\boldsymbol{T}}\boldsymbol{s}_{\boldsymbol{k}} \tag{21}$$

Each column of the leadfield matrix is the steering vector $\boldsymbol{s}_{\boldsymbol{k}}$ of the signal at source K. $\widehat{\boldsymbol{E}}_{\boldsymbol{N}}$ is the estimation of noise eigen vectors since in reality the eigenvectors are not known a-priori and must be estimated from the received signal.

The partitioning of signal and noise subspace is much easier to perform on averaged data, and it may be difficult to implement on online data. In addition, MUSIC assumes white noise and discrete, uncorrelated signals that are less in number compared to the sensors [51].

In practice, two problems usually arise. First, it might be difficult to differentiate “true” from “false” peaks in the MUSIC metric due to errors in estimating the signal subspace. Second, as the dimension of source subspace increases, it becomes difficult to find several local maxima automatically in MUSIC metric [50].

Recent modifications of this methods are performed such as Recursively applied and projected (RAP)-MUSIC to overcome these problems by using a recursive procedure in which each source is located projected out before repeating the scanning procedure [51].

Beamforming is another developed technique, in which data recorded from a sensor array is passed through a spatial filter, which passes signals originated from the location of interest and ideally rejects signals from elsewhere. In brain source localization, the location of interest is scanned throughout the brain and all possible source locations are monitored. Ideally, the spatial filter will pass signals of small distance δ of the location of interest r_q while nulling other signals as [2],

$$\mathbf{W}^T \boldsymbol{K}(\boldsymbol{r}) = \begin{cases} \boldsymbol{I} \ \|\boldsymbol{r} - \boldsymbol{r}_q\| \leq \delta \ ; passband\ constraint \\ \mathbf{0} \ \|\boldsymbol{r} - \boldsymbol{r}_q\| > \delta \ ; stopband\ constraint \end{cases} \tag{22}$$

where $\boldsymbol{W}$ is the spatial filter matrix and $\boldsymbol{K}(r) = [\boldsymbol{k}(\boldsymbol{r}, \boldsymbol{\Theta}_1), \boldsymbol{k}(\boldsymbol{r}, \boldsymbol{\Theta}_2), \boldsymbol{k}(\boldsymbol{r}, \boldsymbol{\Theta}_3)]$ is the lead field matrix for three orthogonal dipoles at location r.

This spatial filtering technique is widely used not only to estimate the location of neuron sources but also to estimate its dynamics without a prior knowledge of the number of active sources [52]. There are two noteworthy drawbacks of beamforming. To start with, it requires an accurate forward solution, which is essential when applied to EEG recordings because of conductivity and anisotropy of the head tissues. Second, the performance of beamforming degrades severely if the sources have the same dynamics e.g. their time-courses of activity are highly correlated within a certain period of time [52]. It is not possible to place a strong stopband filter over the entire brain region because of insufficient degrees of freedom. Hence, a fixed spatial filter for this application is not useful and an adaptive filter is instead used.

Linearly constrained minimum variance (LCMV) beamforming is an implemented adaptive technique that uses a limited number of degrees of freedom to nullify unwanted interfering signals by placing nulls at their positions whereas the desired location is represented with a unity gain constraint [2].

$$\min tr\{C_y\}\ subject\ to\ \mathbf{W}^T \boldsymbol{K}(\boldsymbol{r_q}) = \boldsymbol{I} \quad (23)$$

Where $\boldsymbol{y}$ is the computed output of the beamformer formed as the product of the spatial filter $\boldsymbol{W^T}$ with the signal ***v(t)*** at the array at time *t.* $\boldsymbol{C_y} = E[\boldsymbol{yy^T}] = \boldsymbol{W^T C_v W}$, $\boldsymbol{C_v} = E[\boldsymbol{vv^T}]$. A solution to equation (23) is obtained using the method of *Lagrange multipliers*

$$\mathbf{W} = [(\boldsymbol{K^T}(r_q)\boldsymbol{C_v^{-1}}\boldsymbol{K}(r_q)]^{-1}\boldsymbol{K^T}\boldsymbol{C_v^{-1}} \quad (24)$$

However, LCMV has a number of limitations. The most important one in this application is the localization of sources with correlated signals. In this case LCMV will results in partial cancellation of the signal of interest.

Different approaches have been developed to help in improving source reconstruction of correlated sources. One of the methods is to calculate the second spatial derivative which is called the surface Laplacian (SL) and allows for increased spatial resolution of EEG.

Authors of [52] incorporate the Laplacian forward solution in the EEG LCMV beamforming. In [52] proposed method, the surface Laplacian acts as a filter that allows spatial separation of sources which overlap in raw scalp EEG recordings.

Lately, spatiotemporal beamforming methods have been proposed for localization of instantaneous or evoked brain responses. In [53] an event-related beamformer (ERB) algorithm was applied to localize source power throughout the brain for individual interictal spike data. They described the use of ERB as a new tool for source localization of interictal discharges in patients with intractable neocortical epilepsy.

3.4.3 Distributed Sources Dipole Model

Another commonly used approach to solve the inverse problem is the distributed source model. It is assumed that multiple sources can be simultaneously active at any given time and across many locations. It is worth mentioning that this method does not require an *a priori* assumption on the number of dipoles. Cerebral activity is reconstructed at each point in the solution space. Each point represents a mini-dipole, these dipoles have fixed positions but their orientations and strength vary. However, an infinite number of dipole combinations can lead to the generation of a similar scalp potential map. Therefore, distributed models require further assumption in order to identify the optimal or most likely sources [46].

One of the most recently developed methods to localize multiple distributed cortical sources is low resolution electromagnetic tomography (LORETA). It is based on the assumption that neighboring neural populations are likely to undergo synchronous depolarization during an evoked response or a discharge than the non-neighboring neurons.

The generalized problem of LORETA is expressed mathematically as in [54],

$$\min F_w \qquad where\ F_w = \|\boldsymbol{V} - \boldsymbol{KJ}\|^2 + \alpha \boldsymbol{J}^T \boldsymbol{WJ} \tag{25}$$

the Tikhonov parameter $\alpha > 0$ is the control parameter and $\boldsymbol{W}$ is the weight matrix that is used to implement the spatial Laplacian operator, the solution to equation (25) is,

$$\hat{\mathrm{J}} = \boldsymbol{T}_W \boldsymbol{V} \tag{26}$$

where $\boldsymbol{T}_W = \boldsymbol{W}^{-1}\boldsymbol{K}^T(\boldsymbol{K}\boldsymbol{W}^{-1} + \alpha \boldsymbol{H})^+$. $\boldsymbol{H}$ is average reference operator and defined as

$\boldsymbol{H} = \boldsymbol{KT}$ where $\boldsymbol{T}$ is the generalized inverse of the leadfield matrix $\boldsymbol{K}$.

The generated solution is blurred since the neighborhood sources are assumed to have similar strength. LORETA provides smooth and better localization for deep sources with less localization error. However, spatial resolution is relatively low.

An advanced version of LORETA is the standardized LORETA (sLORETA) in which current distribution throughout brain volume is computed. Also, the biological variance in the actual signal and the variance of EEG measurement noise are taken into account [48].

sLORETA can be expressed mathematically as in [55],

$$\min F_J \qquad where\ F_J = \|\boldsymbol{V} - \boldsymbol{KJ}\|^2 + \alpha \|\boldsymbol{J}\|^2 \tag{27}$$

The source estimation is

$$\hat{\mathrm{J}} = \boldsymbol{T}_J \boldsymbol{V} \tag{28}$$

where $\boldsymbol{T}_J = \boldsymbol{K}^T(\boldsymbol{K}\boldsymbol{K}^T + \alpha \boldsymbol{I})^{-1}$. Although sLORETA algorithm can correctly localize sources, the produced image is also blurred.

Further development is made to minimize localization error by choosing weight matrix to give more importance to deep sources. Exact LORETA (eLORETA) provides the exact localization with zero error in presence of measurement and biological noise. But, still it suffers from low spatial resolution just as LORETA and sLORETA [48].

Another high-resolution estimation method is the Source Affine Image Reconstruction (SAFFIRE) algorithm which is the neuroimaging application of the adaptive Re-iterative super-resolution (RISR). RISR is based on the recursive implementation of the MMSE solution. It is also based on assuming that the collected measurement can be modeled as a superposition of independent contribution from arbitrarily distributed sources. The received EEG signal measurements as in equation (16)

$$\boldsymbol{y}(\mathrm{n}) = \boldsymbol{S}\boldsymbol{x}(n) + \boldsymbol{v}(n) \tag{29}$$

Basically, SAFFIRE searches for an adaptive filter bank that minimizes the following cost function,

$$f = \mathrm{E}\{\|\boldsymbol{x}(n) - \hat{\boldsymbol{x}}(n)\|^2\} = \mathrm{E}\{\|\boldsymbol{x}(n) - \boldsymbol{W}^{\boldsymbol{T}}(n)\boldsymbol{y}(n)\|^2\} \tag{30}$$

where $\hat{\boldsymbol{x}}(n)$ is the MMSE estimate of $\boldsymbol{x}(n)$. The minimization of the cost function f is found by taking its derivative with respect to $\boldsymbol{W}$ and equating it to zero,

$$\mathrm{E}\{2\boldsymbol{y}(n)\,[\boldsymbol{x}(n) - \boldsymbol{W}^{\boldsymbol{T}}(n)\boldsymbol{y}(n)]\} = 0 \tag{31}$$

therefore,

$$\boldsymbol{W}(\mathrm{n}) = (E\{\boldsymbol{y}(n)\boldsymbol{y}^{\boldsymbol{T}}(n)\})^{-1}E\{\boldsymbol{y}(n)\boldsymbol{x}^{\boldsymbol{T}}(n)\} \tag{32}$$

Substituting equation (32) in (29) with assuming that source amplitudes and noise are uncorrelated, the filter bank is found to be [56],

$$\boldsymbol{W}(\mathrm{n}) = (\boldsymbol{S}E\{\boldsymbol{x}(n)\boldsymbol{x}^{\boldsymbol{T}}(n)\}\boldsymbol{S}^{\boldsymbol{T}} + E\{\boldsymbol{v}(n)\boldsymbol{v}^{\boldsymbol{T}}(n)\})^{-1}\boldsymbol{S}E\{\boldsymbol{x}(n)\boldsymbol{x}^{\boldsymbol{T}}(n)\} \tag{33}$$

$$\boldsymbol{W}(\mathrm{n}) = (\boldsymbol{S}\boldsymbol{P}\boldsymbol{S}^{\boldsymbol{T}} + \boldsymbol{R}_{\boldsymbol{v}})^{-1}\boldsymbol{S}\boldsymbol{P} \tag{34}$$

where $\boldsymbol{P}$ is the spatial power distribution and $\boldsymbol{R}_{\boldsymbol{v}}$ is the noise correlation matrix. $\boldsymbol{R}_{\boldsymbol{v}}$ can be determined from the time samples of a baseline, however $\boldsymbol{P}$ is not known a-priori and must be estimated using matched filter bank initializations [56]:

$$\hat{\boldsymbol{X}}_{\boldsymbol{o}} = \boldsymbol{S}^{\boldsymbol{T}}\boldsymbol{Y} \tag{35}$$

$$\hat{\boldsymbol{P}}_{\boldsymbol{o}} = E\left\{\hat{\boldsymbol{X}}_{\boldsymbol{o}}\hat{\boldsymbol{X}}_{\boldsymbol{o}}^{\boldsymbol{T}}\right\} \odot \boldsymbol{I}_{K\times K} \tag{36}$$

where, $\odot$ is the Hadamard product, and $\boldsymbol{I}$ corresponds to the identity matrix which makes sources temporally uncorrelated.

Non-coherent Integration. To solve temporal correlation issue, the algorithm operates on each time sample individually or the power estimates are combined through non-coherent integration. The iterative steps of the SAFFIRE algorithm is as follows:

In order to determine *N* source amplitudes, the aggregate filter bank is in equation (34)

$$\overline{\boldsymbol{W}}(\mathrm{n}) = (\boldsymbol{S}\overline{\boldsymbol{P}}\boldsymbol{S}^{\boldsymbol{T}} + \boldsymbol{R}_{\boldsymbol{v}})^{-1}\boldsymbol{S}\overline{\boldsymbol{P}} \tag{37}$$

the initialization is done as in equations (35) and (36). Then, the estimations of source amplitudes and average spatial power distribution for N time samples are,

$$\widehat{\boldsymbol{X}} = \overline{\boldsymbol{W}}^{\boldsymbol{T}}\boldsymbol{Y} \tag{38}$$

$$\overline{\boldsymbol{P}} = \frac{1}{N}\sum_{\tau=0}^{N-1}\widehat{\boldsymbol{X}}(n+\tau)\widehat{\boldsymbol{X}}(n+\tau)^{\boldsymbol{T}} \odot \boldsymbol{I}_{K\times K} \tag{39}$$

Equations (37), (38) and (39) encompass the SAFFIRE algorithm iterative steps which converge in 15 iterations. The number of sources, their amplitudes and locations are estimated via the peaks of $\widehat{\boldsymbol{X}}$. The estimate of the amplitude distribution can be obtained from the diagonal elements of the matrix $\sqrt{\overline{\boldsymbol{P}}}$.

The main advantages of SAFFIRE are that it can operate on very low sample support and can determine the number of sources automatically. Furthermore, it does not require eigen decomposition and it offers good robustness temporal correlation.

To summarize, several studies have shown that EEG source imaging has made an extremely good progress to provide neurophysiological interpretation of scalp recordings. The first step in estimating the sources underlying electric fields at the scalp is the analysis of these electric fields where both temporal and spatial dimension of brain activity are considered simultaneously.

In general, EEG is a noninvasive technique with high temporal resolution in comparison with other functional techniques such as PET and fMRI along with low hardware cost [57]. Moreover, multichannel EEG systems have become affordable for all clinical and research laboratories. Notably, EEG is a direct method to measures brain's electrical activity unlike other methods which are indirect markers for activity in the brain and it can measure neuronal activity in real time when investigating temporal properties of the brain.

On the other hand, EEG spatial resolution is relatively poor since the measurements taken by each electrode are in fact the sum of electric field produced by a large number of neurons, which yield in detecting strong electrical activity by neighboring electrodes as well. As a result, the exact source of activity using EEG is difficult to determine.

Chapter 4. Experimental Data

4.1 Data Overview

A dataset [58] containing EEG data was used to demonstrate source reconstruction of the N170 ERP of face perception.

ERP relates recorded signal with stimulus events, which is done by focusing on the change in the electrophysiological signal immediately after the stimulus event [59]. ERP waveforms are described in terms of positive and negative peaks (to be more specific, the most positive and the most negative deflections in the wave). The naming for ERP components can be identified by the sequence in which the peak occurs with the polarity being indicated. For example, N1 and P2 indicate the first negative peak and the second positive peak in the waveform respectively. Moreover, labeling can also identify the positive and negative peaks by their latency. On the other hand, a functional description of ERP peaks refers to their physiological interpretation, which, in general, identify specific cognitive processes reflected by each peak. In addition to the latency measurements and functional interpretation, ERP descriptors include topographical scalp distributions or identify electrodes where maximum amplitudes are observed.

N170 refers to the negative peak that occurs 170 milliseconds following stimulus onset, and it is associated with the visual processing of human faces. The topographic distribution of the N170 component for both familiar and unfamiliar faces is the largest over the occipitotemporal regions [60-63].

The demonstration below involves localizing the N170 using the distributed source method, LORETA. The EEG data were acquired on a 128 channel, sampled at 2048 Hz in addition to two channels, to measure HEOG and VEOG. The 128 channels are divided into four groups and every 32 channels measure electric potentials of a specific area in the scalp. These channels are named A (Back), B (Right), C (Front), and D (Left).

To proceed with the data analysis and ERP extraction, Advanced Source Analysis (ASA) lab software was used to analyze EEG signals and reconstruct sources using different source localization functions. ASA-lab software is a complete system used to acquire and analyze EEG/MEG signals.

4.2 Data Pre-processing

As a first step towards analyzing, EEG data was loaded to ASA-Lab along with electrode positions file that contains the coordinates of each electrode sensor position. A standard head model and MRI images were also used in the analysis. Next, Artifact activity was determined manually and corrected by spatial filtering to separate brain signals from artifacts based on their topography and remove it without altering brain signals. Principle Component Analysis (PCA) method was used to determine topographies of the artifact signals and the artifact-free brain signals. PCA is a statistical procedure that converts a set of observations with correlated variables into a set of linearly orthogonal variables called principle components. EEG epoch is decomposed into components that model either brain or artifact activity where each component consists of a waveform and a topography vector. The waveform describes the time course of the modeled activity whereas the vector describes how waveform contributes to each recorded signal. From a large artifact-free subset of the data segment to be corrected, brain signal topographies are determined by a relevant number of principle components topographies. The subset is obtained by automatically excluding sample vectors from the original data segment if they exceed a certain amplitude in one or more channels or exceed a specific correlation with the vector space spanned by the predefined artifact topographies. In Amplitude criterion, artifacts with amplitudes above the normal amplitude range of EEG are identified. The correlation criterion can detect sample vectors of artifact that have not been identified by the amplitude criterion in which the similarity between the measured topography and the predefined tomography is calculated, and a correlation threshold is set. When decomposing by PCA, only the first p of PCA topographies sorted from highest to lowest explained variance are used as the brain activity estimation, where p is a particular number that has to be determined empirically [64].

Artifact correction was performed as follows. First, a number of segments of the recorded EEG was selected and classified visually as artifact activity as in Figure 4-1. These segments were used to specify artifact topography. Then, the mean of selected data interval was used to achieve the separation. At the end, artifact components were removed as shown in Figure 4-2.

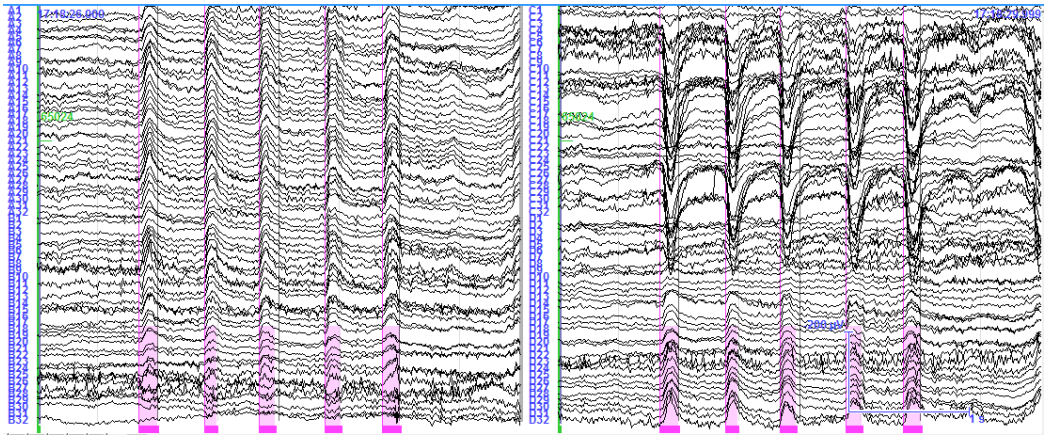

Figure 4-1 Highlighted window specifies artifacts events.

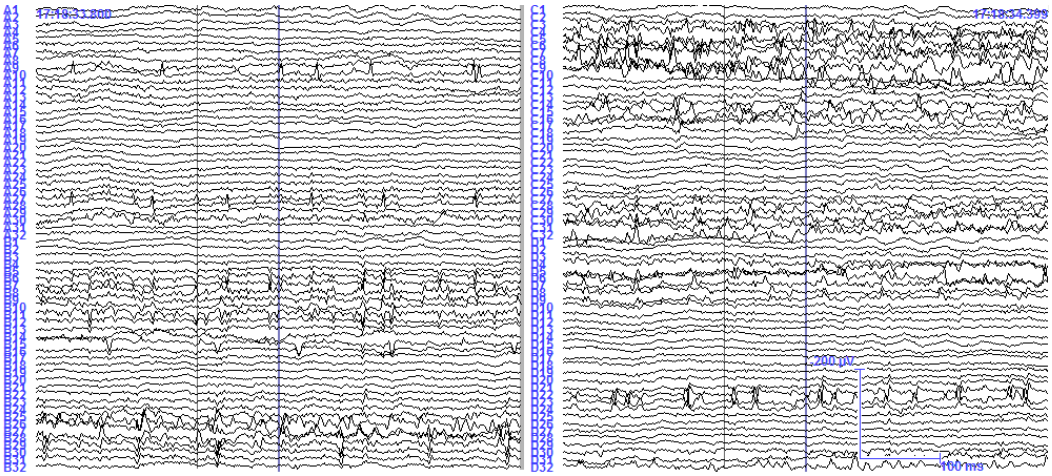

Figure 4-2 EEG data after artifact correction.

After the artifact correction, the EEG signal was passed through high pass and low pass filters in series with cut-off frequencies 0.5 Hz and 30 Hz respectively. The filtered EEG signal is shown in Figure 4-3.

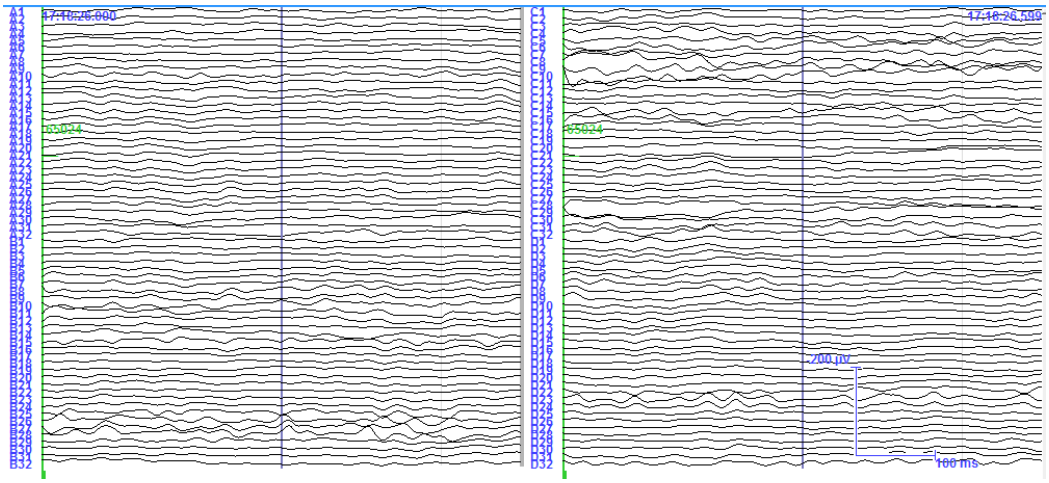

Figure 4-3 EEG signal after passing through lowpass and high-pass filters.

The paradigm involved the presentation of 172 faces and 172 scrambled faces; hence, these events were labeled to represent stimulus conditions using the conditioning method in ASA-lab. The final step in processing the data was averaging EEG sections, which are defined by events or conditioning markers.

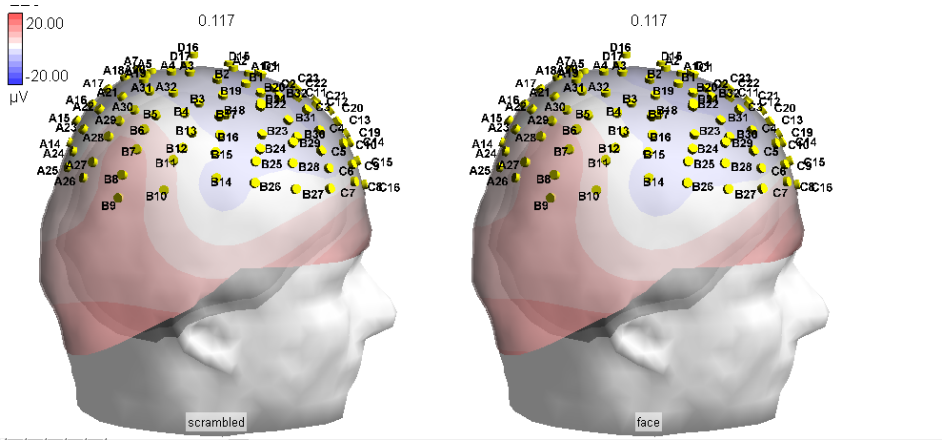

Figure 4-4 Voltage map of the averaged events at time 117 milliseconds.

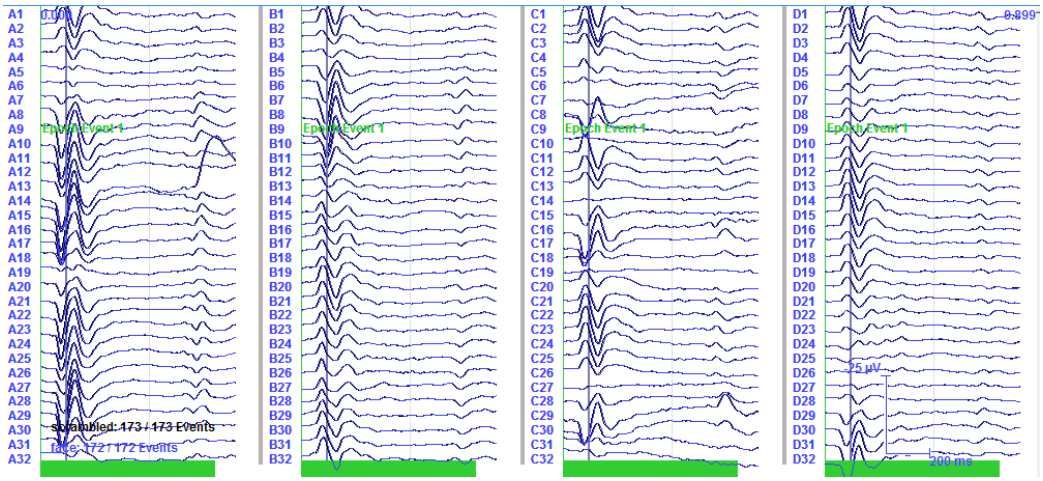

Figure 4-5 EEG data view of averaged events.

Figure 4-5 represents the averaged events across each channel which are clear ERP signals. For example, if we displayed the extracted ERP signal at channel D12 as in Figure 4-6, it is obvious that the negative peak is at 160 milliseconds.

4.3 Forward Problem Solution

As mentioned previously in this report, an appropriate forward solution is required to solve the inverse problem accurately. Basically, a volume head conductor model is assumed to represent the sources' activity in the brain.

The forward problem was obtained using ASA-lab software. An individual MRI image was used and anatomical landmarks were used to define a head-based

coordinate frame or other locations in the MRI. Nasion, left ear, and right ear markers were required to define head-based coordinate frame for the MRI. After that, the MRI image was split into head compartments (scalp, skull, brain) as in Figure 4-7.

Figure 4-6 ERP at channel A28.

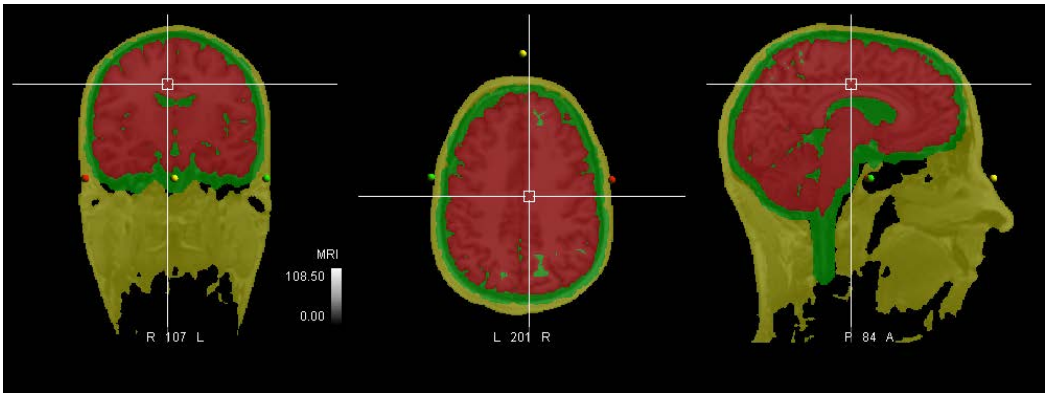

Figure 4-7 MRI segmentation of scalp, skull and brain.

The next step after the segmentation of head compartments is to generate a realistic head model. As mentioned before, the realistic head model takes into account the different conductivities of the head compartments. The technique used for head modeling is Boundary Element Method (BEM). The lead-field matrix was computed at the end of head model generation procedure.

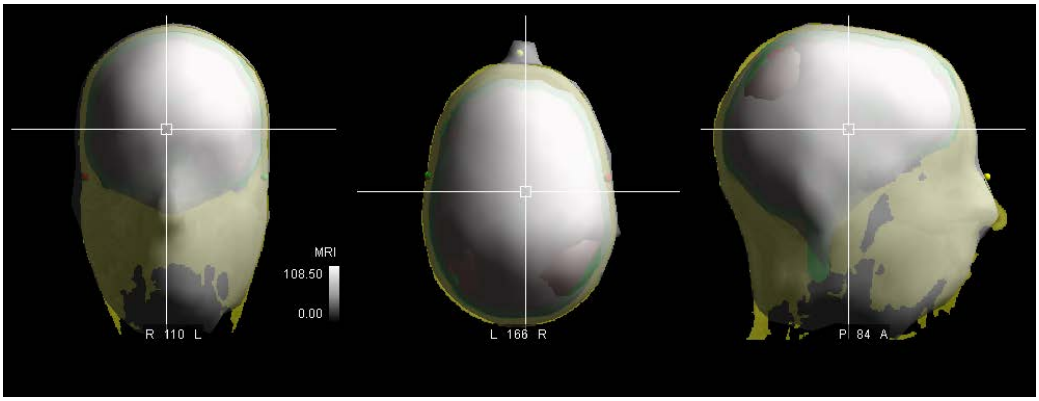

Figure 4-8 Head model using BEM.

4.4 Inverse Problem Solution

LORETA source localization was used to reconstruct sources of the N170 EEG signal for a single subject.

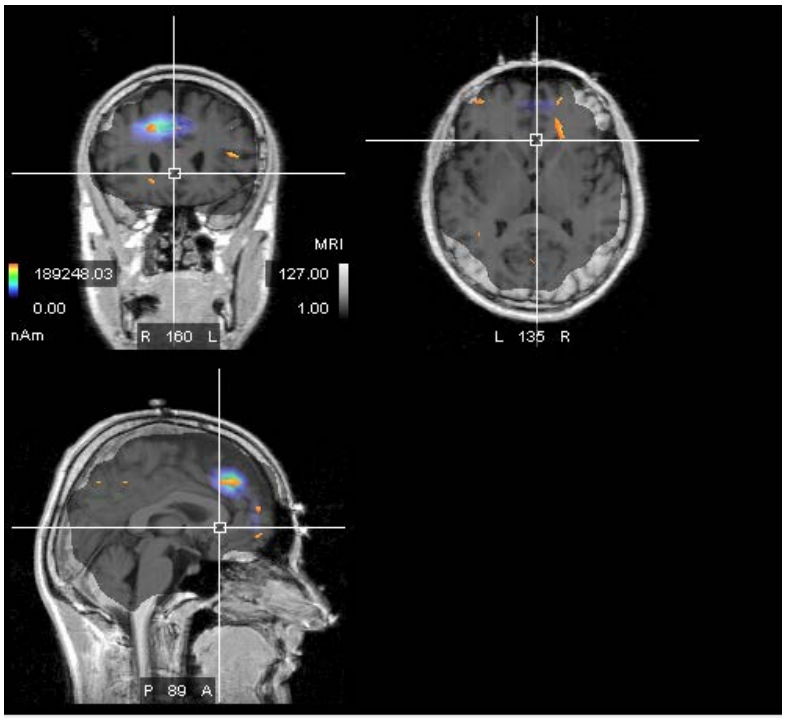

Figure 4-9 Visualization of Source localization results.

Sources are illustrated as arrows with different lengths and orientations to represent dipoles. The dipole is activated and displayed as a source by comparing the activation magnitude of each dipole with the magnitude exhibited by its 16 nearest neighbors. When none of these neighbors has a magnitude higher than that of the dipole, then this dipole is activated. Figure 4-9 represent sources reconstructed using LORETA algorithm.

4.5 Discussion

As shown in *Figure 4-9*, the most dominant activated dipoles were located in the frontal area and they all correspond to the event of displaying face. As known, the frontal region is responsible for cognition activity in the brain. However, as mentioned earlier, N170 distribution is dominant in the occipitotemporal region. By investigating the data set, we found that the two events (face and scrambled) carry the exact same data and can be clearly shown in *Figure 4-5*. This can be due to an error in labeling events or a redundancy in data since the total number of both events is 172 as in [58] and events' labels should be updated as the condition label file. Also, the electrode locations present in the dataset were based on channel labels and may not be precise enough. It may even be completely wrong because sometimes electrodes are not placed in the correct locations for the corresponding channel labels. Hence, this can be corrected by importing individually measured electrode locations.

Chapter 5. Source Localization with Exact Knowledge of the Leadfield Matrix

5.1 Simulated Data

Simulated EEG signals were produced for a 256-electrode system. The distributed sources space was obtained from a subject's structural T1-weighted MRI with Freesurfer. It consists of a mesh of the 8000 vertices. Dipoles were located at each vertex and oriented radially to the surface [65].

The forward problem solution was obtained in a 3-layer realistic head model using the Boundary Element Method (BEM) implemented in Brainstorm software. The EEG simulations were generated from a single network located in the inferior parietal region. A total number of 30 epileptic spikes were simulated in 20 epochs of 60 s at 512 Hz as shown in Figure 5-1. Furthermore, the simulated data was imported to brainstorm for sources analysis.

To solve the inverse problem, two source localization algorithms, sLORETA and SAFFIRE, were applied to the non-averaged spikes EEG signal in order to locate the sources with the largest power spectrum peaks.

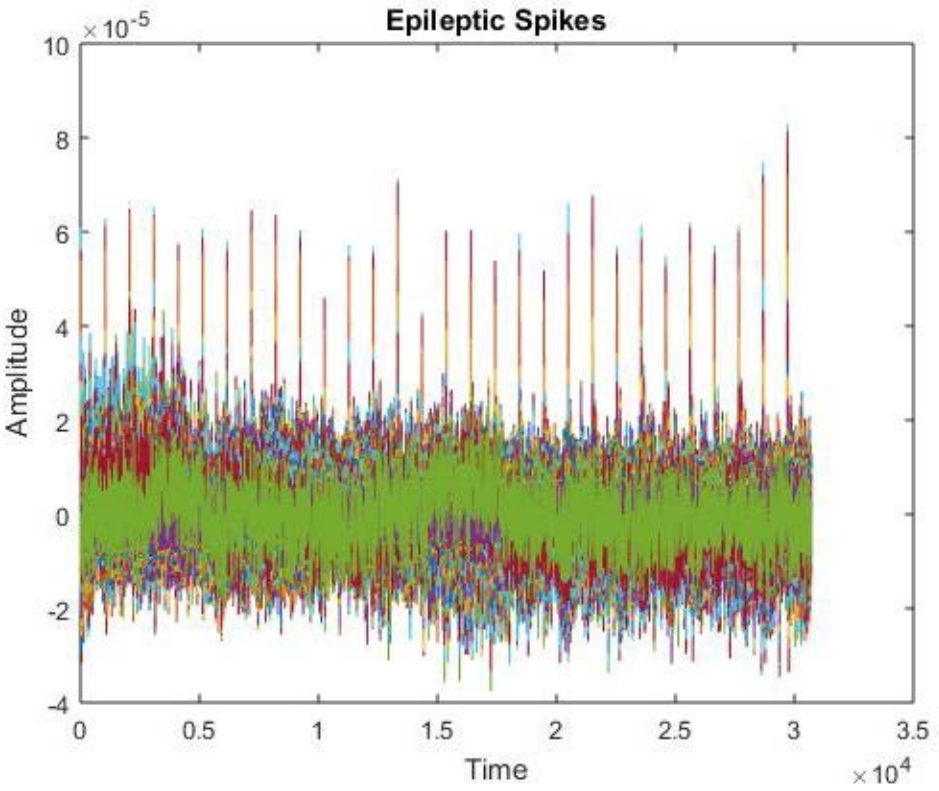

Figure 5-1 Simulated Epileptic spikes.

5.1.1 Source Localization using SAFFIRE

The SAFFIRE Algorithm was applied on the simulated epileptic spikes with the knowledge of the exact Leadfield matrix. Figure 5-2 shows the obtained SAFFIRE power spectrum.

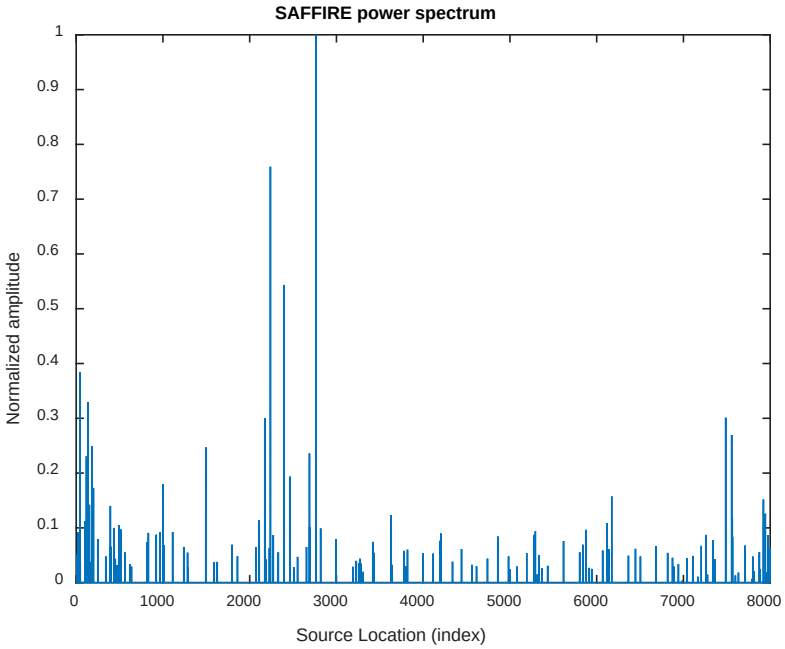

Figure 5-2 SAFFIRE power spectrum of sources for simulated epileptic spikes.

A threshold of 0.25 was applied in order to find the strongest sources amongst them. Figure 5-3 displays the strongest sources plotted in red that were located in the left parietal region as in [65]. The blue sources displayed in Figure 5-3 are the actual (ground truth) region that has been used to simulate epileptic spikes.

Due to the randomness of the detected sources, localization error will be calculated from the mean of the detected sources and the mean of the ground truth. Figure 5-4 demonstrates the mean of the true location as a blue dot whereas the mean of the detected sources as a red dot.

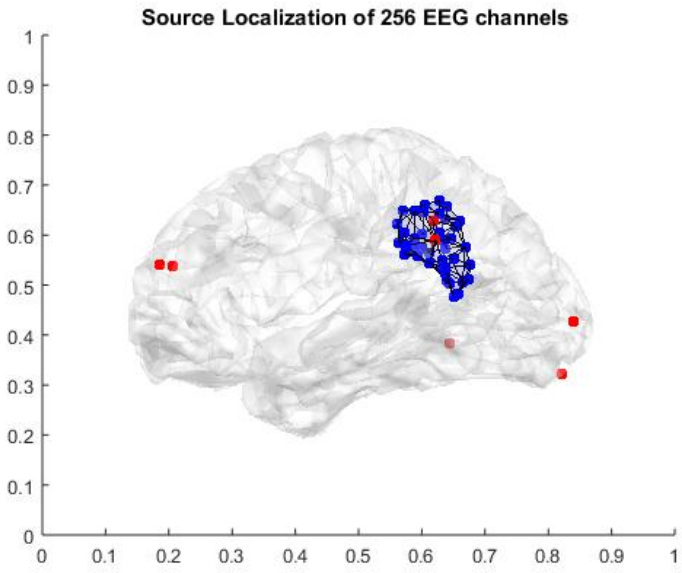

Figure 5-3 The strongest detected active sources along with the true locations of sources.

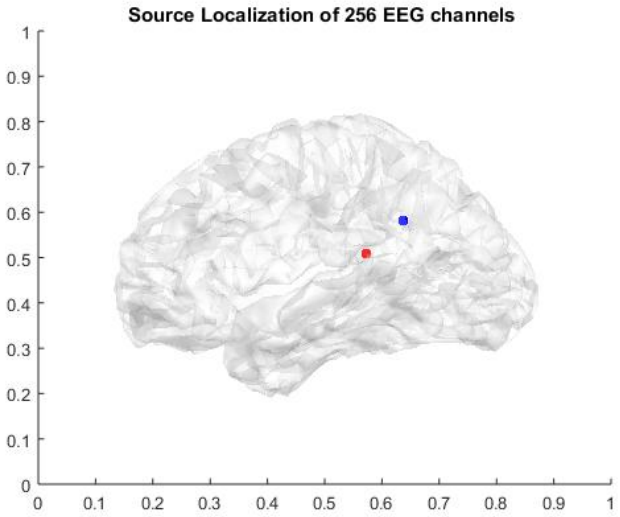

Figure 5-4 The mean of detected active sources along with the mean of true locations of sources.

5.1.2 Source Localization using sLORETA

sLORETA algorithm was obtained on the time of epileptic peaks. First, the most energetic signal was selected to find peaks locations. Figure 5-5 and Figure 5-7 show the signal with maximum energy recorded by channel CP5 and the epileptic peaks respectively. On the other hand, Figure 5-6 shows 256 electrodes in yellow and the one in red which recorded the most energetic signal.

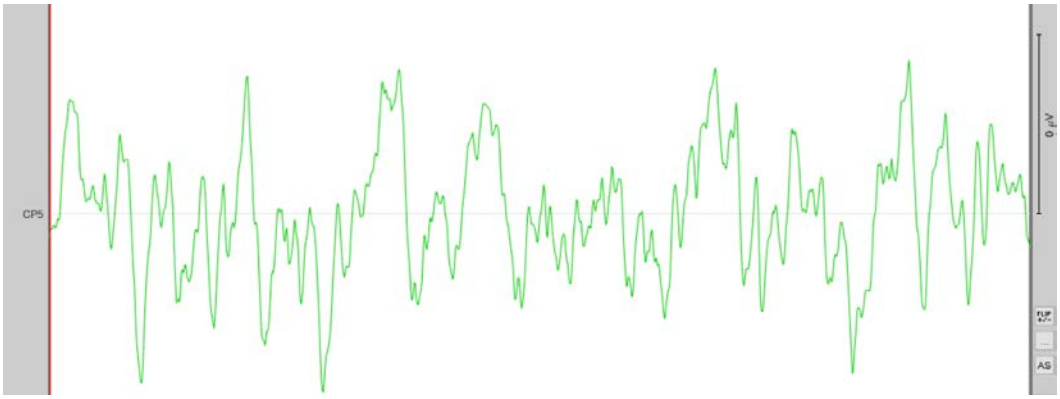

Figure 5-5 The signal with the maximum energy.

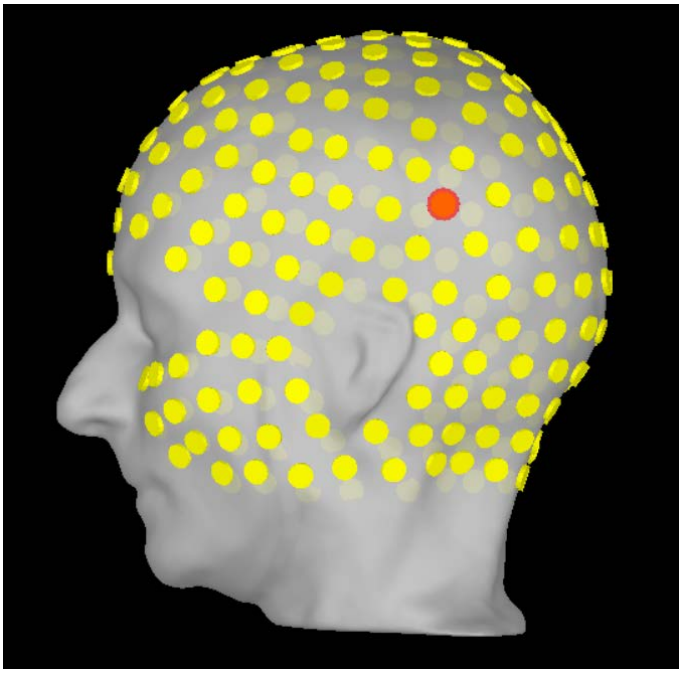

Figure 5-6 256 electrodes system projected on the head model

Next, BEM was used to generate a realistic head model. The sLORETA function was applied to the simulated epileptic data using Brainstorm software. A back and a left side views of source mapping on cortex are displayed in Figure 5-8 and Figure 5-9 respectively at one of the peaks times found from the previous step. The ground truth is mapped with a red circle in Figure 5-9.

As a step towards calculating source localization error, the power spectrum of the sources was used to select sources with the highest power. Next, the mean of the detected sources was calculated as well as the mean of the ground truth.

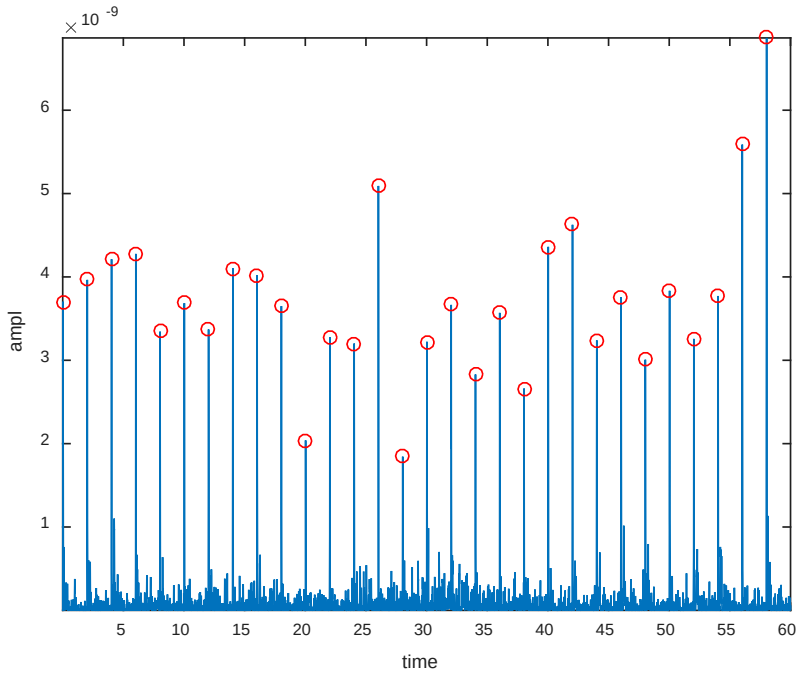

Figure 5-7 The 30 peaks in the most energetic signal.

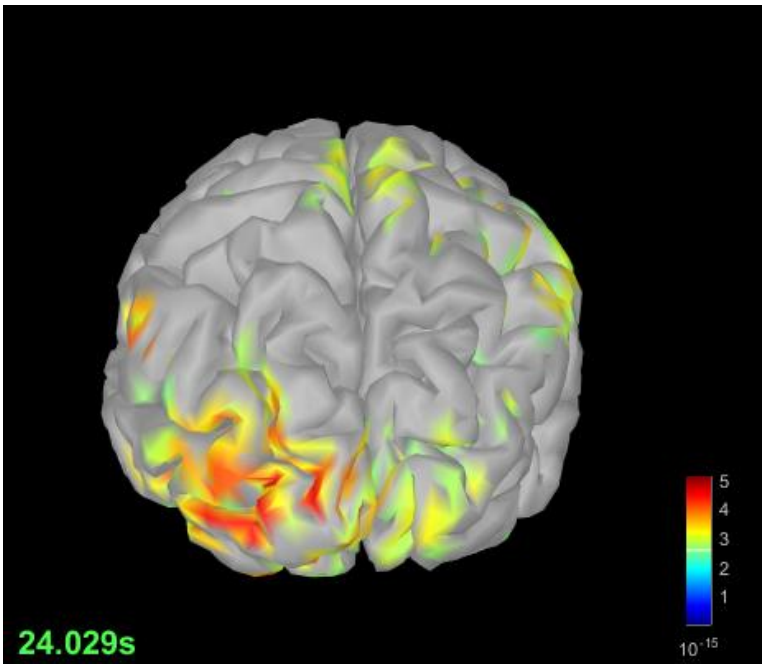

Figure 5-8 sLORETA source localization mapping on cortex at peak time 24.029 s.

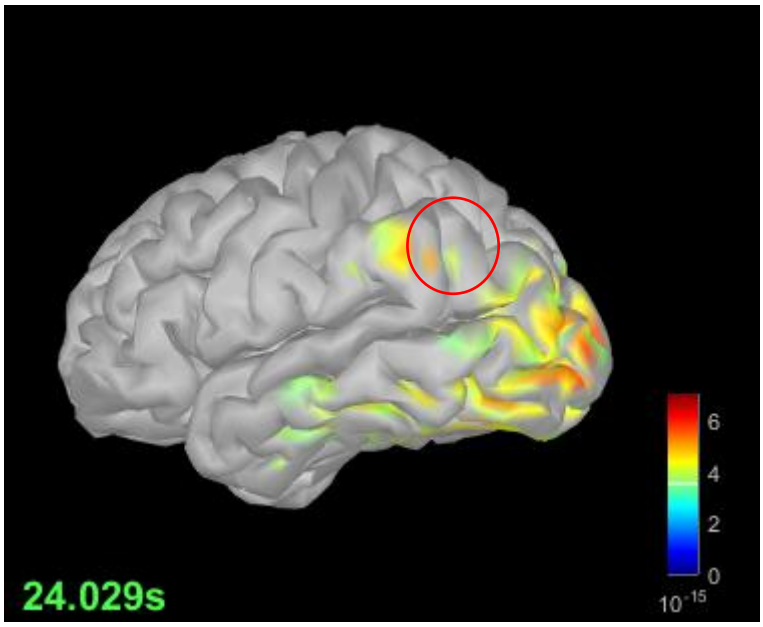

Figure 5-9 Side view of sLORETA mapping at peak time 24.029 s.

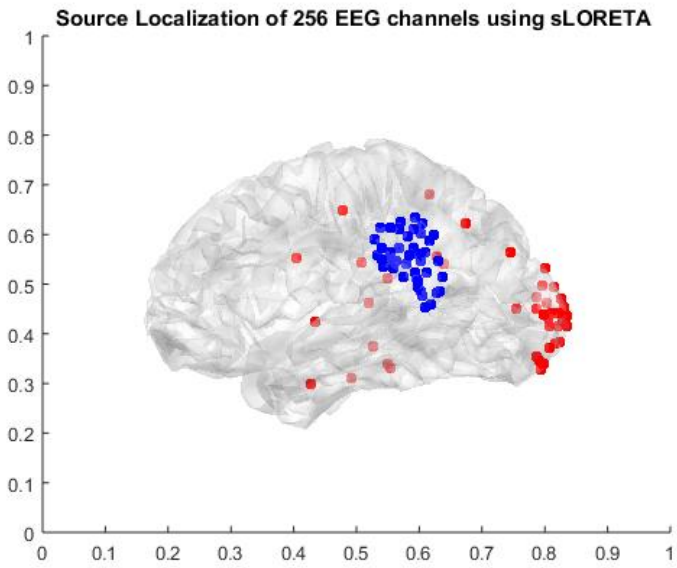

Figure 5-10 The strongest detected active sources along with the true locations of sources.

5.1.3 Discussion

By comparing sLORETA and SAFFIRE results, it was found that both resulted sources were consistent and map the same regions, However, when comparing these detected regions and the actual true regions, sLORETA resulted in a source localization error of 6.25 cm from the mean of the ground truth whereas SAFFIRE source localization error was 3.55 cm. Therefore, localization using SAFFIRE was more efficient since it is a high-resolution algorithm as mentioned in section 3.4.3. It is worth to note that this localization error will decrease to 7.44 mm when

thresholding for higher powers and considering the highest power sources resulted from SAFFIRE algorithm.

5.2 Experimental Data

The real epileptic data in [65] were collected from a patient during pre-surgical evaluation for drug-resistant focal epilepsy. The MRI showed a focal cortical dysplasia in the mesial aspect of the orbitofrontal region. Dense-256 channels EEG was recorded for 1 h, at 1000 Hz. A total of 85 spikes were selected visually after artifacts correction. The sources of interictal spikes were spread over the left frontal and temporal regions as displayed in Figure 5-11. Source localization using sLORETA and SAFFIRE was applied on averaged spikes shown in Figure 5-12. Realistic head model was also obtained in brainstorm using Boundary Element Method before solving the inverse problem.

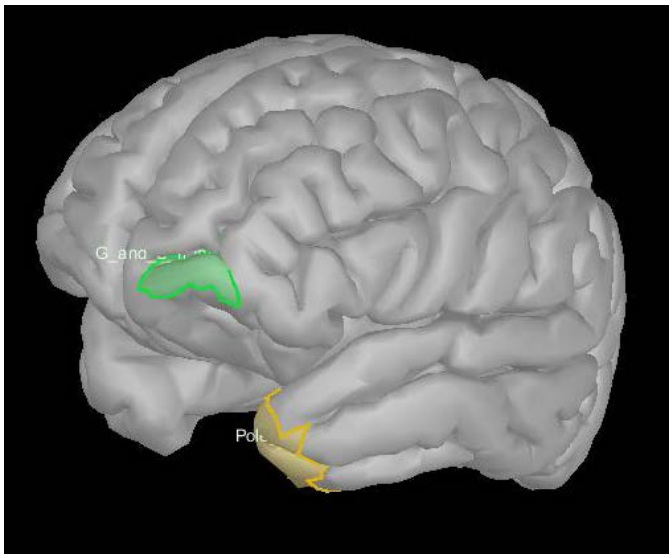

Figure 5-11 Left frontal and temporal poles regions on cortex.

5.2.1 Source Localization using SAFFIRE

The SAFFIRE Algorithm was applied to the real epilepsy data and the used leadfield matrix was assumed to be accurate. The power spectrum of the sources was obtained as in Figure 5-13. In order to determine the strongest active sources, a threshold of 0.2 was applied.

The detected sources of scalp EEG recordings were plotted in blue on the cortex as in Figure 5-14. The highest activity sources were located the left frontal and temporal regions. Also, sources with substantial activation were detected in right frontal poles as in [65].

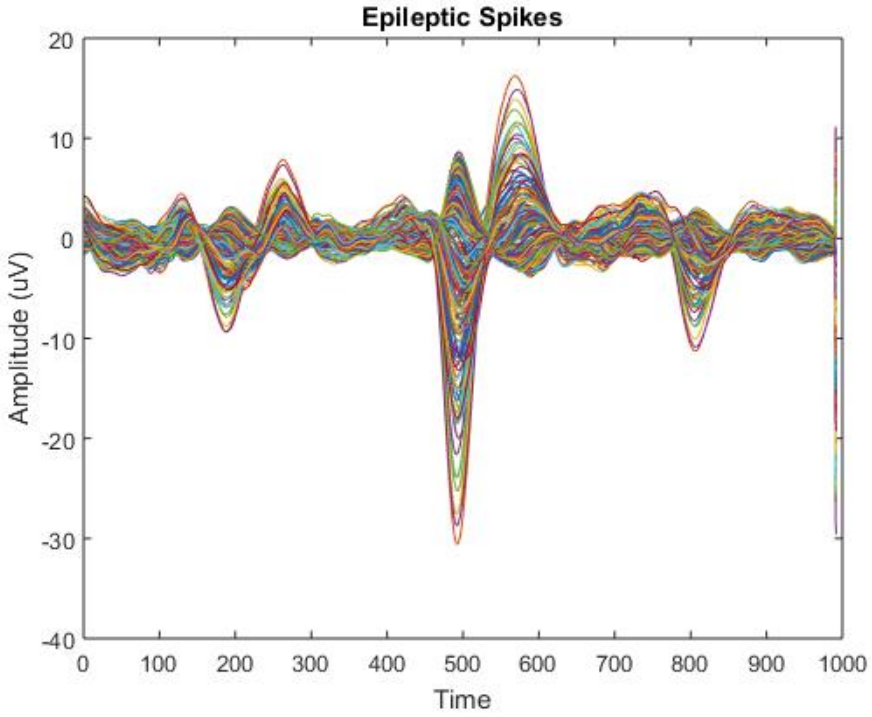

Figure 5-12 Averaged real epileptic data.

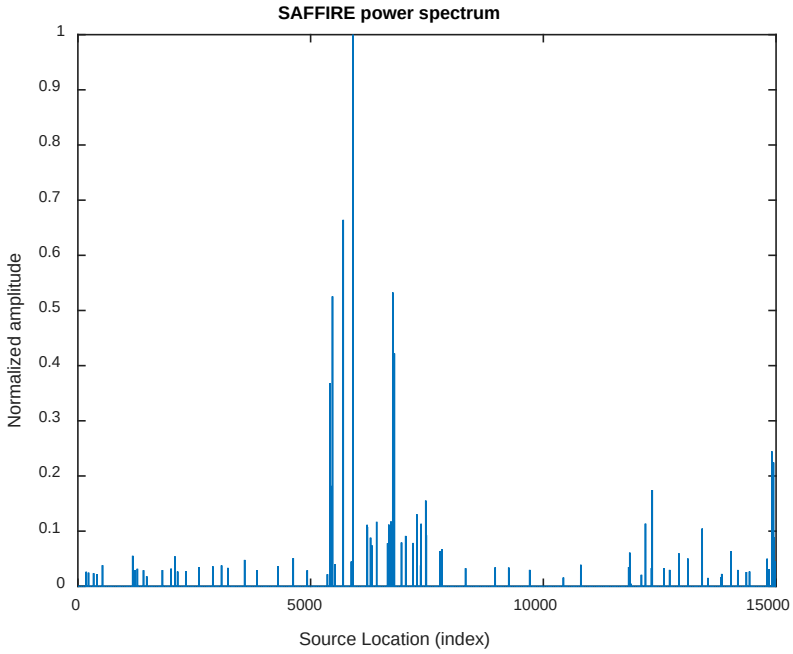

Figure 5-13 SAFFIRE power spectrum of real epileptic spikes.

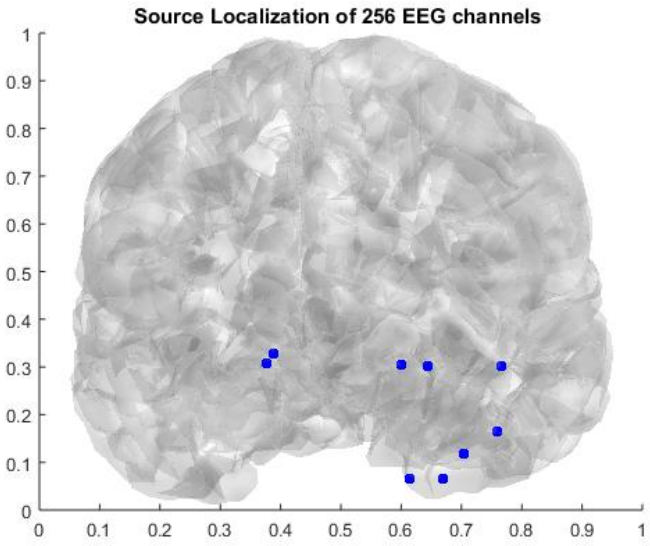

Figure 5-14 The strongest active sources resulted from SAFFIRE algorithm for real epileptic spikes.

5.2.2 Source Localization using sLORETA

In order to perform sLORETA algorithm, Brainstorm software was used. Subject's MRI image and electrodes position file were uploaded to the software. Next, BEM was used to generate a 3-layer realistic head model. Noise covariance was estimated from a baseline data recorded for 1 s. Sources were estimated for the averaged real data described in Figure 5-15 which displays the epileptic spikes that were generated from left frontal and temporal regions. The maximum sources' activation were found in frontal and orbitofrontal regions whereas sources with less or substantial activation were found in left temporal and right frontal regions as [65].

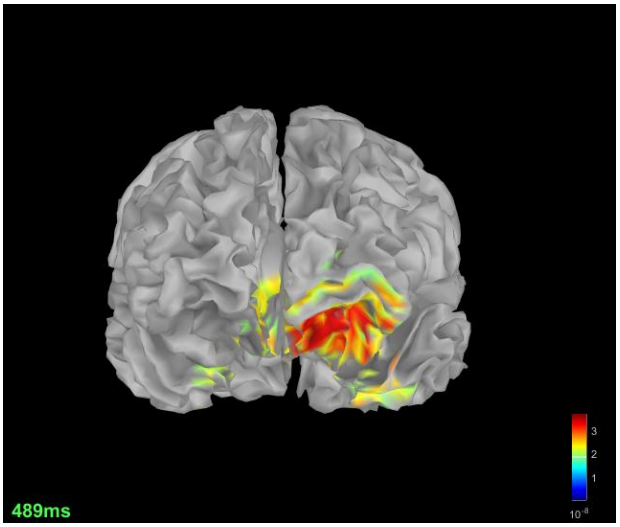

Figure 5-15 Front view of sLORETA source localization mapping on cortex for real data.

5.2.3 Discussion

As concluded in section 5.1.3, source localization error when using SAFFIRE algorithm is much less than using the sLORETA algorithm to solve the inverse problem. Hence, detected sources resulted from SAFFIRE algorithm can be thought of as the ground truth of multifocal epileptic zone to calculate the performance of sLORETA algorithm since the exact location of sources vertices is unknown.

In order to find the source localization error for the sLORETA algorithm, the power spectrum density generated from Figure 5-15 with a threshold of 0.5 was compared with SAFFIRE power spectrum in Figure 5-13 to find the sources' locations in brain cortex.

Due to the randomness of the detected sources, a statistical analysis of the mean and variance is obtained to calculate the source localization error when applying the sLORETA algorithm. An error of 29.05% was found for detecting left frontal sources. On the other hand, 84.9% and 24.98% error for detecting left temporal and right frontal sources respectively.

The normalized power of each source was thresholded by keeping the indices with highest strength values. This procedure was used to detect the sources of the maximum activity using the two inverse methods. Different threshold values were used to study the effect of this threshold. It was found that higher threshold values will increase right frontal and left temporal source localization errors for both SAFFIRE and sLORETA inverse methods and both methods will not be able to detect right sources.

Chapter 6. Epilepsy Source Localization

As mentioned before, EEG is the most important tool in the diagnosis and management of epilepsy. However, it must be properly performed and carefully interpreted by experienced specialists to provide an accurate assessment. EEG recordings have been used to localize epileptogenic regions for pre-surgical evaluation and are used to identify specific physiological abnormalities. The presence of signal change on interictal and ictal EEG can be good predictors of the epileptogenic zone for surgical resections purposes. Therefore, we sought to estimate epileptogenic zone using SAFFIRE source localization algorithm to validate epileptogenic zones suggested by specialists.

6.1 Patients and Data Acquisition

Three medically diagnosed patients with focal epilepsy were studied for source localization as approved by Rashid Hospital at Dubai. All EEG recordings were carried out using the 10-20 international electrode system. Figure 6-1, Figure 6-2 and Figure 6-3 display recorded EEG for the three patients respectively with some labeled spikes. Neurologists had specified the epileptogenic foci for each patient along with other neurological abnormalities after investigating the EEG records.

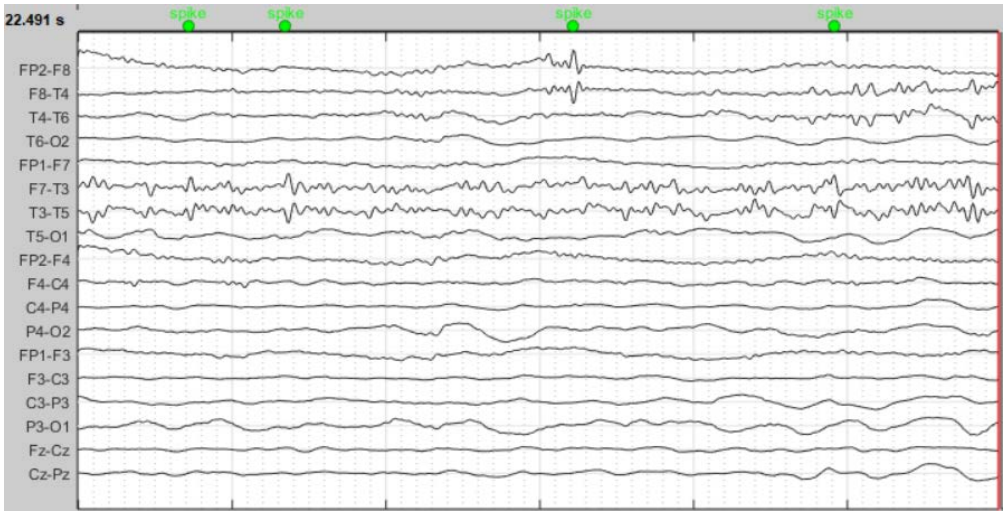

Figure 6-1 EEG recording of patient 1 with some spikes labelled in green.

Figure 6-2 EEG recording of patient 2 with some spikes labelled in green.

Figure 6-3 EEG recording of patient 3 with some spikes labelled in green.

6.2 Clinical Data Analysis

Distributed sources dipole was calculated using SAFFIRE algorithm. BEM was used to obtain a realistic head model as a step to solve the forward solution. The generated head model is composed of three layers that represent the scalp, skull, and brain as demonstrated in Figure 6-4, it was obtained using a standard MRI image due to the unavailability of MRI images of each patient.

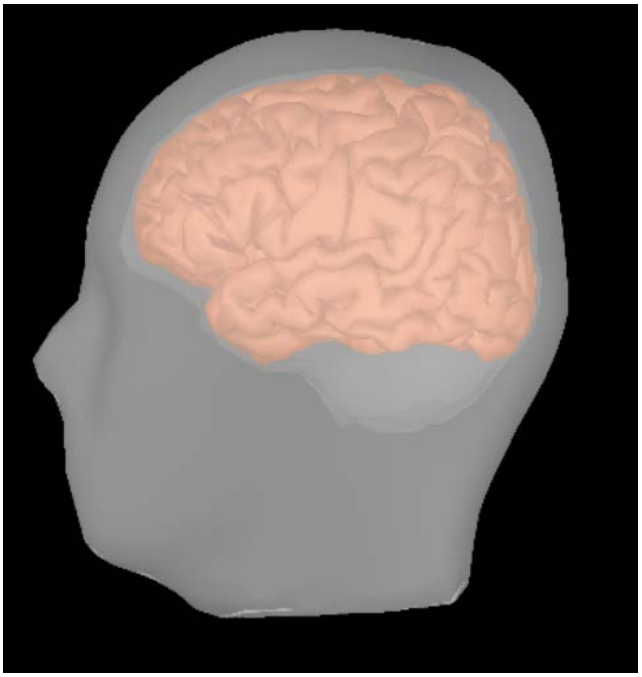

Figure 6-4 realistic 3-layer head model.

Figure 6-5 shows the standard electrode cap that has been used in the EEG analysis since the actual electrode positions were not available

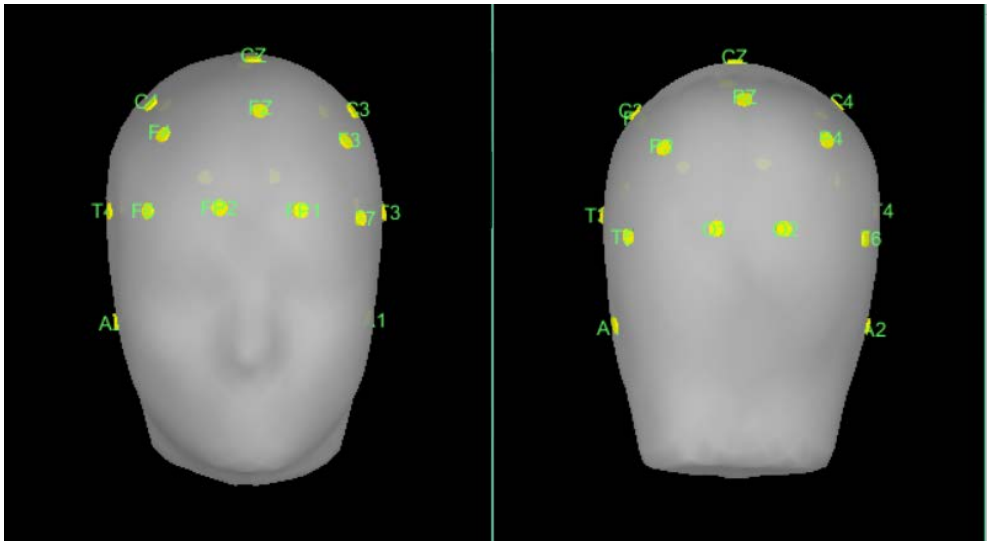

Figure 6-5 Projected electrodes on head.

After solving the inverse problem, the sources that correspond to the maximum signals were projected to the cortical surface to determine the epileptogenic foci. Figure 6-6 shows the main four lobes of the human brain cortex.

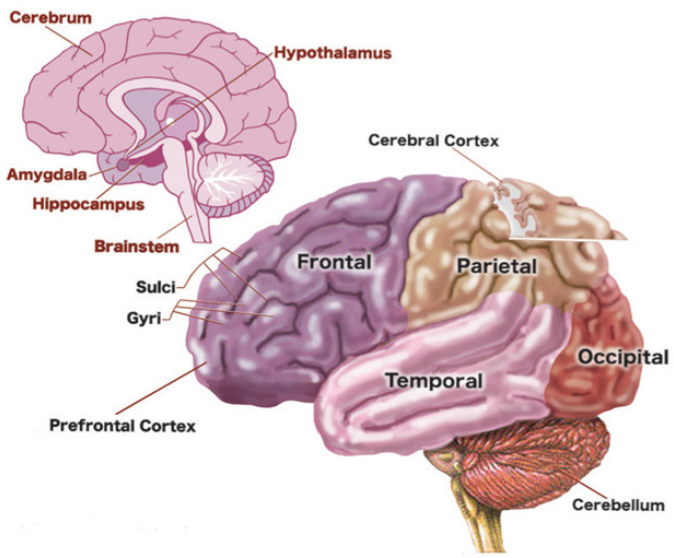

Figure 6-6 Cerebral cortex lobes in the brain.

6.3 Results

It was necessary to determine if the inverse solution of SAFFIRE algorithm for locating epileptogenic foci is similar to the medical diagnoses done by neurologists for each patient. Therefore, the SAFFIRE algorithm was applied to the EEG recording of each patient after generating the head model and the lead-field matrix (solving the forward problem). For patient 1, the clinical interpretation suggested a tendency for focal epilepsy with the left frontotemporal potential epileptogenic focus. SAFFIRE normalized power generated by each source is shown in Figure 6-7. A Threshold of 0.2 was applied to map the sources with the highest power.

The reconstructed maximum sources were mapped to the cortical as in Figure 6-8 where the detected sources were in a bilateral front region. As a side note, the detected sources with maximum power were active in the left frontal region as suggested by the neurologist.

Patient 2 EEG recordings showed focal bilateral fronto-centro-temporal epileptiform discharges. The same procedure was performed to the EEG data and the resulted normalized power generated by each source after applying SAFFIRE algorithm on the recorded EEG is shown in Figure 6-9. In this case, a Threshold of 0.1 was used to map the sources with the highest power which were scattered in the fronto-central temporal regions as reported in the medical report of this patient.

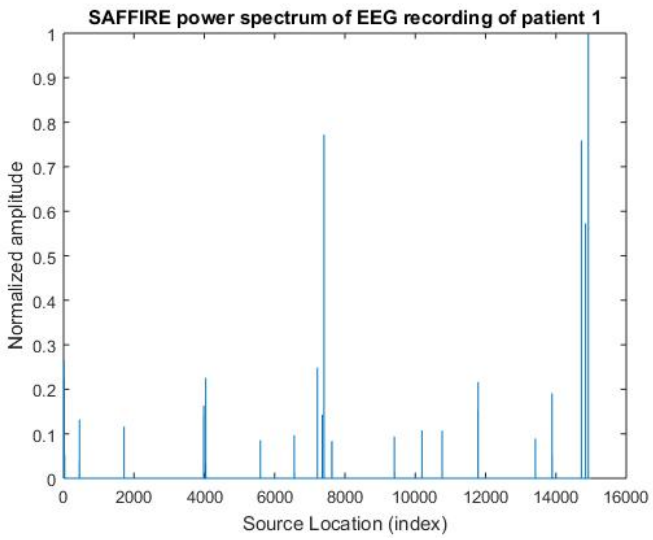

Figure 6-7 SAFFIRE power spectrum of EEG recording- patient 1.

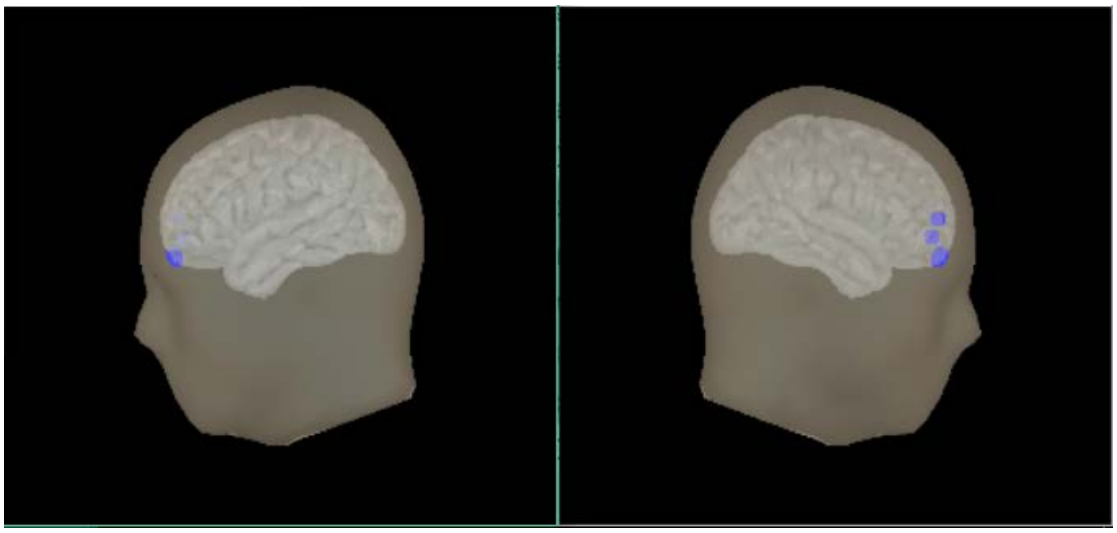

Figure 6-8 Epilepsy source localization for patient 1.

However, for a higher threshold, the sources were mapped to bilateral frontotemporal regions as in Figure 6-10. It is worth to mention that there were active sources corresponds to visual activity as reported by neurologists, and hence it was expected to have sources mapped in the occipital region since it is the center of visual processing.

For patient 3, the clinical interpretation of EEG record shows focal bilateral frontotemporal epileptiform discharges. Figure 6-11 illustrates SAFFIRE normalized power generated by each source. A Threshold of 0.4 was used to map the sources with the highest power.

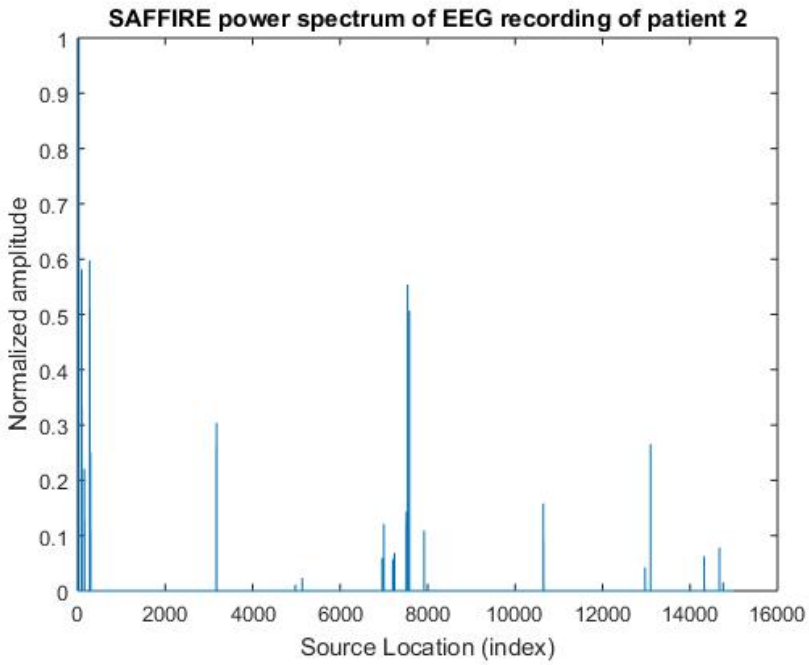

Figure 6-9 SAFFIRE power spectrum of EEG recording - patient 2.

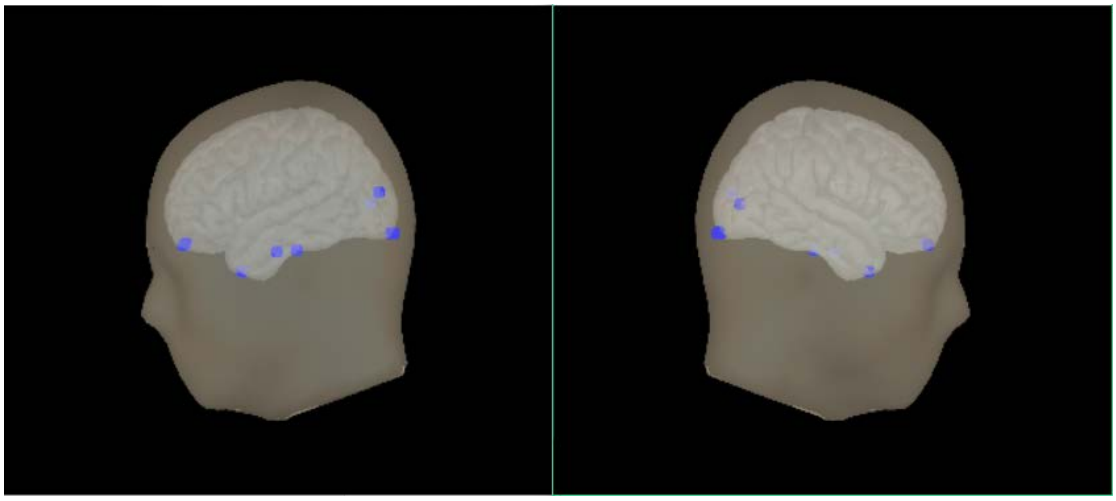

Figure 6-10 Epilepsy source localization for patient 2.

The detected sources were mapped to brain cortex and as demonstrated by Figure 6-12, they were scattered in the bilateral frontal lobes with one active source in the occipital region that could be due to a visual activity.

The threshold is then increased to 0.6 and the maximum power sources were active in the frontal region only as illustrated in Figure 6-13.

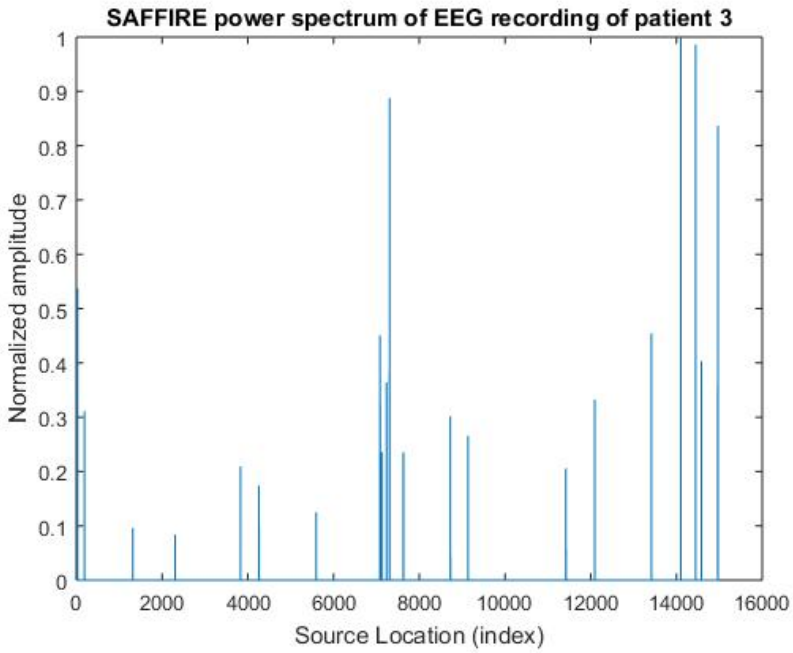

Figure 6-11 SAFFIRE power spectrum of EEG recording - patient 3.

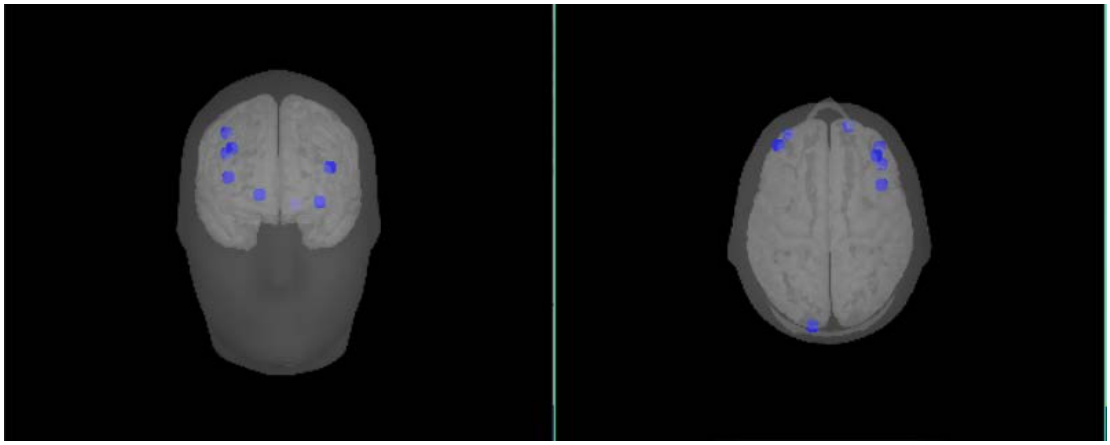

Figure 6-12 Epilepsy source localization for patient 3 – power threshold 0.4.

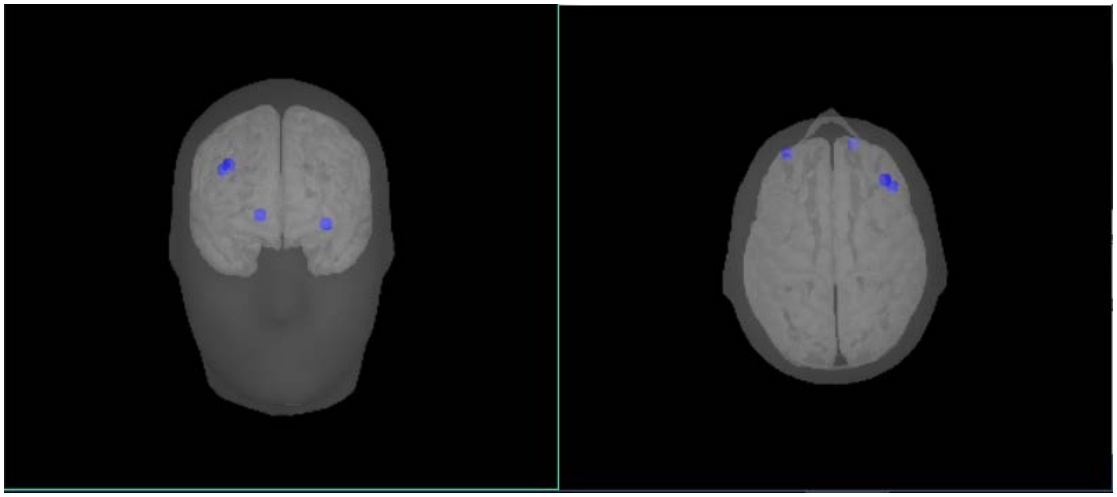

Figure 6-13 Epilepsy source localization for patient 3 – power threshold 0.6.

6.4 Discussion

Our results validate that EEG recordings have an important role in localizing epileptogenic regions. It also revealed that it is possible to determine the location of epilepsy source using the SAFFIRE estimation algorithm. The localized epileptogenic foci were consistent to the suggested locations by neurologists and may even be more precise. However, these localized regions can be more accurate if the provided EEG was perfectly tailored to the need of localization. In other words, physicians should have the knowledge about EEG features that are only related to epileptic seizures during the examination. For example, epilepsy spikes should be marked by physicians during examination and reported with all related information. These events should be used in the analysis and pre-processing of EEG records so that the results do not misinterpret with other abnormalities than epilepsy. Providing that the EEG is technically correct and made for the purpose of localization, the most important factor that affects localization results is the obtained head model. Although a realistic BEM head model was used, localization would be more accurate if an exact head model that is generated from patient's MRI image was used. Moreover, the exact electrode locations for each patient may be a factor that helps in increasing localization accuracy.

In conclusion, it was shown that SAFFIRE estimation algorithm has succeeded to localized epileptogenic regions using EEG recordings and gave reasonable accurate results that were consistent with the medical records. A further improvement in source localization can be done by providing the above mentioned missing data and better analysis of EEG recordings.

Chapter 7. Sensors Dimensionality Reduction Effect on Epileptic Source Localization Performance

As mentioned in chapter 3, The use of EEG source localization can aid in presurgical evaluation in epilepsy patients. Many researches have conducted experiments to study the efficiency of using EEG for epilepsy source analysis and it has indicated the capability of localizing epileptogenic regions with acceptable precision using EEG.

Accurate forward and inverse solutions are considered to be successful steps toward better performance and reduced localization error. However, one major concern is determining the minimum number of electrodes to prevent poor performance. This issue has been studied in previous researches as [66] that concluded an improvement in source localization as the number of electrodes increased. However, there is still a need to relate clearly the localization error and the number of EEG electrodes and determine the number of electrodes required for accurate localization [66].

In this chapter, the localization error is inspected when the number of electrodes is reduced from 256 electrodes down to 32 electrodes. The localization error is calculated based on the statistical mean of the true location of sources and the mean of detected localized sources using different electrodes number.

7.1 Data Analysis

The simulated epilepsy data used in section 5.1 was also used in this performance study. Starting from 256 EEG recording, the 128 subset electrodes were selected by comparing electrodes labels and ANT Neuro EEG cap naming scheme. The scalp potential recordings for the selected electrodes were used. SAFFIRE method was used to calculate the inverse solution of the distributed dipole model using an updated normalized leadfield matrix by selecting only the steering vectors that correspond to the selected electrodes. In order to calculate the source localization error, the distance between the mean of the true location of sources and the mean of the reconstructed sources.

The same procedure was repeated to reduce sensor dimensionality from 128 down to 64, and 32 electrodes.

7.2 Results

Since the SAFFIRE algorithm was performed for each dataset individually, it was necessary to consider all sources of significant power and then average the location of the detected sources.

Starting with applying SAFFIRE on the selected 128 EEG channels, sources with power higher than 0.25 of the maximum power were considered as detected sources. The mean of the detected sources and the mean of the ground truth were plotted on cortex as in Figure 7-2 and used to calculate source localization error.

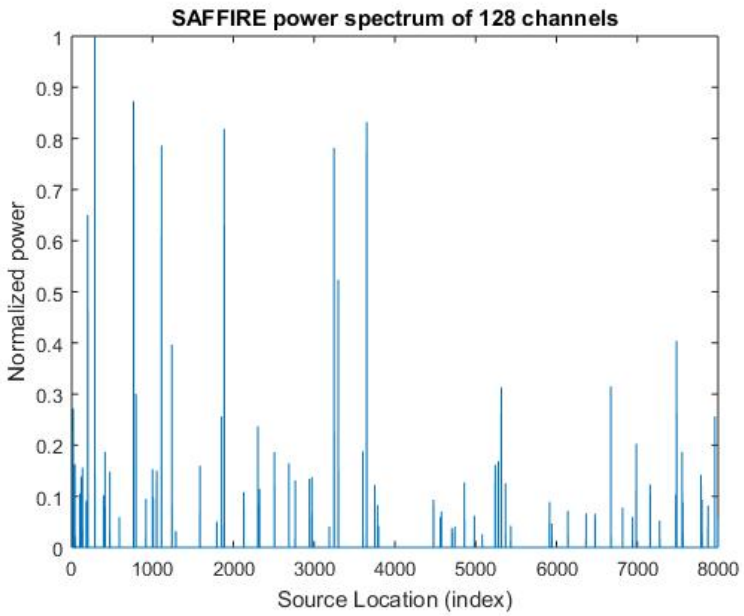

Figure 7-1 SAFFIRE power spectrum of 128 channels.

Next, 64 EEG channels were selected from the 128 channels. The potential recorded by these channels were applied on SAFFIRE with the corresponding steering vectors from the leadfield matrix. Figure 7-3 and Figure 7-4 show SAFFIRE power spectrum and the mean location of the detected source respectively.

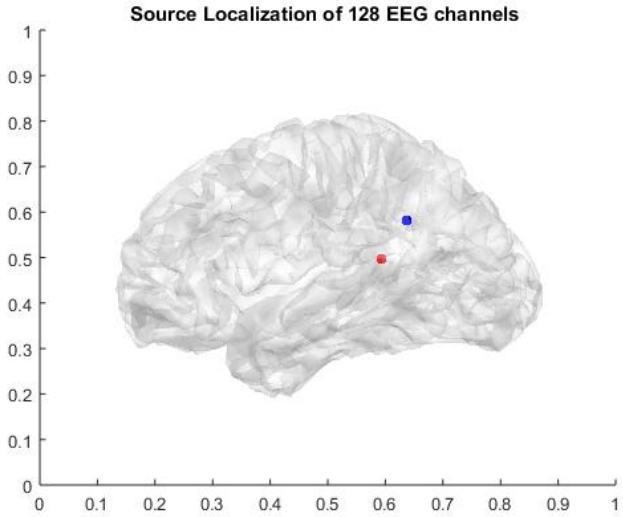

Figure 7-2 The mean of detected active sources from 128 Ch. along with the mean of true locations of sources.

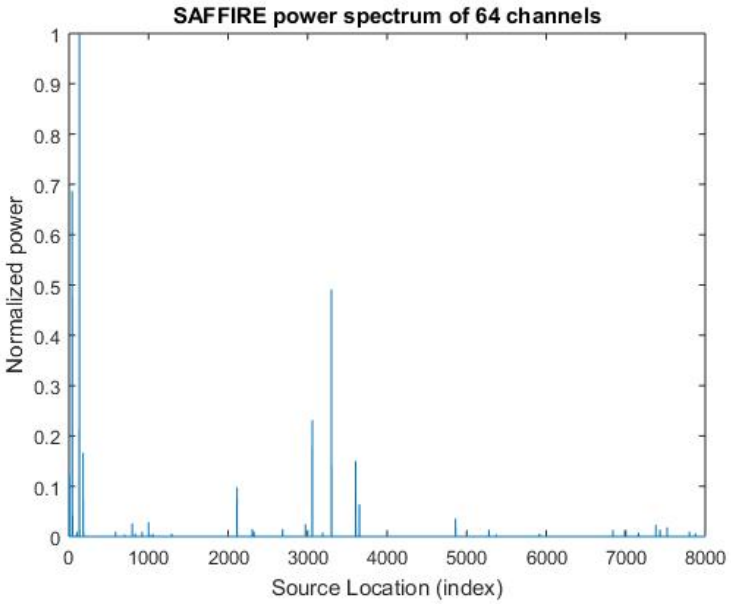

Figure 7-3 SAFFIRE power spectrum of 64 channels.

By repeating the above-mentioned procedure, 32 EEG channels were selected also according to ANT Neuro naming scheme. Figure 7-5 and Figure 7-6 show SAFFIRE power spectrum resulted from 32 EEG channels and detected sources mean plotted on brain cortex respectively.

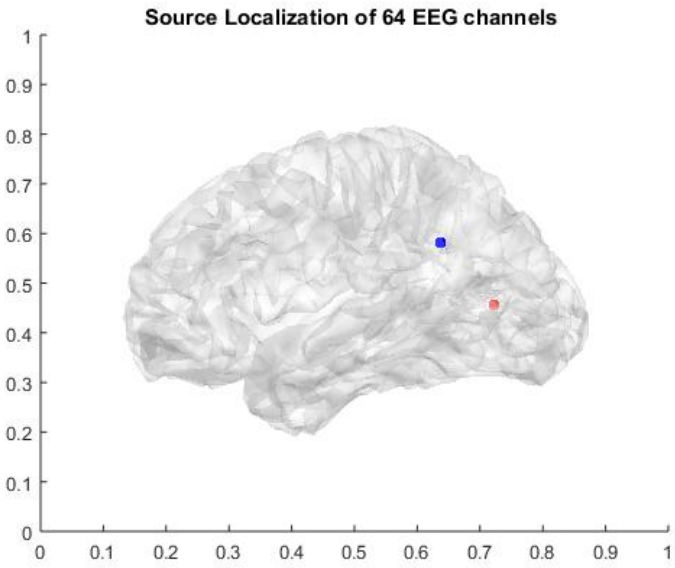

Figure 7-4 The mean of detected active sources from 64 Ch. along with the mean of true locations of sources.

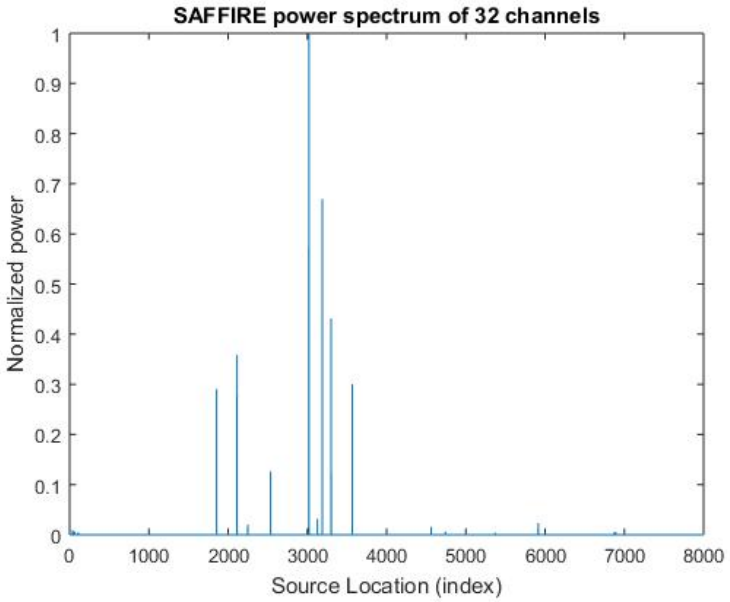

Figure 7-5 SAFFIRE power spectrum of 32 channels.

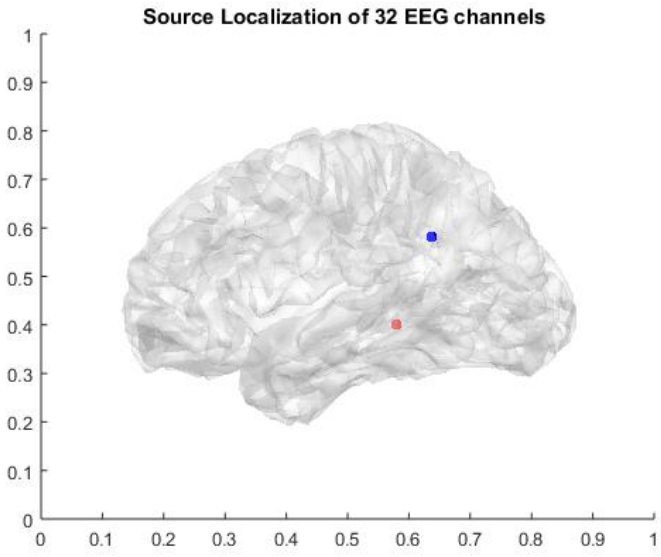

Figure 7-6 The mean of detected active sources from 32 Ch. along with the mean of true locations of sources.

7.3 Discussion

The relationship between the number of electrodes and epilepsy source localization error have been examined for a simulated data of epileptic spikes. As it can be seen from Figure 7-7, the source localization error for the simulated epileptic data had generally increased when the number of electrodes decreased. The most dramatic increase can be seen when reducing the number of electrodes from 256 down to 128 where the localization error increased by 2.18 cm. Then it increased by 3.7 mm when going from 128 electrodes to 64 electrodes. However, localization error decreased by 5.1 mm when reducing the number of electrodes to 32 electrodes.

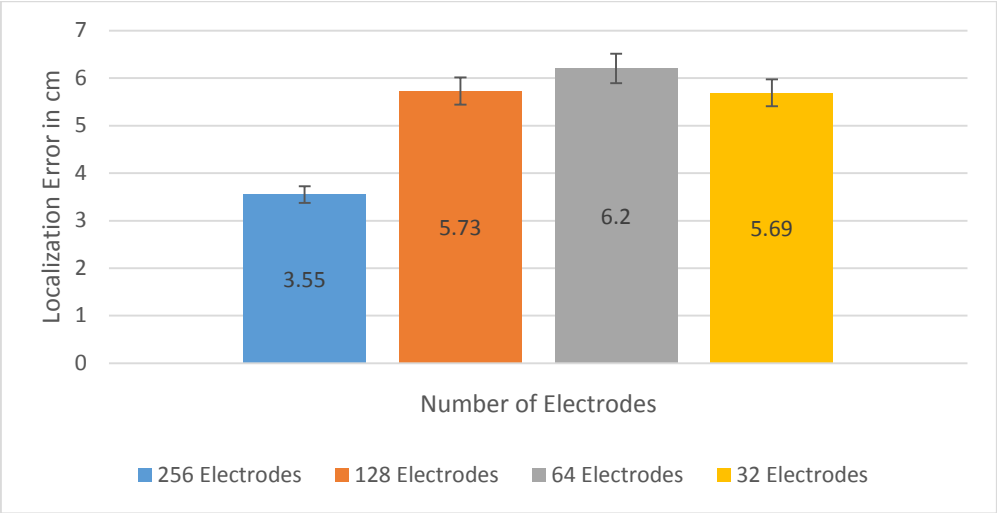

Figure 7-7 Source Localization Error for different electrode numbers.

The effect of noises on EEG channels is not uniform, this may be the reason behind the reduction in source localization error for 32 electrodes system. One way to improve source localization error is to find the channels that are least affected by noise. A system in [67] is represented to analyze EEG signals and avoid channels averaging by finding the least affected channels by noise and reduce the number of channels.

Moreover, the relationship between localization error and electrode numbers can be investigated by performing a series of simulations and clinical data analysis for a number of patients. Another way to improve the localization error calculations is to perform error analysis on each spike individually then average the localization errors.

Chapter 8. Conclusion and Future Work

8.1 Conclusion

The main focus of this thesis is to investigate source localization algorithm in epilepsy as it is the most common neurological disorder. Different imaging techniques that are used to diagnose epilepsy are addressed and compared together. Electroencephalography (EEG) was chosen since it is the most common imaging technique and considered to be a direct method to measure brain's electrical activity with high temporal resolution in comparison with other functional techniques. The first step in estimating the sources underlying electric potentials on the scalp is the analysis of these electric fields. Then, solving the forward problem and obtaining a head model that resembles patient's head. After that, sources are detected by assuming a distributed source model and solving the inverse problem.

SAFFIRE algorithm was used in this thesis for the purpose of epilepsy source localization. This iterative algorithm assumes that the collected measured potentials can be modeled as a superposition of independent contribution from a number of sources distributed arbitrarily. The iterative steps estimate source power distribution. The performance of SAFFIRE algorithm was compared with sLORETA in the knowledge of exact source locations of a simulated epilepsy data. The detected sources resulted from SAFFIRE algorithm were considered to be more accurate than detected sources by the sLORETA algorithm. Also, the algorithm was tested on clinical EEG data collected from three patients in order to determine epileptogenic foci for each case. The strongest detected sources were mapped in brain regions that are consistent with the clinical interpretation suggested by neurologists.

The final part of this thesis investigated the effect of reducing electrodes number on epilepsy source localization error. SAFFIRE algorithm was applied to a simulated data and the number of electrodes was reduced from 256 to 128 and from 128 to 64 and finally to 32. The source localization error of simulated data generally increased when the number of electrodes decreased. However, as mentioned earlier this relationship can be affected by EEG channel noises and needs more investigations on series of simulations and clinical data to confirm the trend.

8.2 Future Work

This research work can be extended in various ways. Although the used algorithms in this thesis resulted in a reasonable epilepsy source localization,

algorithms performance can be improved by using an exact lead-field matrix and further analysis of EEG records before applying algorithms. Further investigations on the localization of epileptic regions using SAFFIRE algorithm for EEG data of epilepsy patients can be done. Collected EEG data from hospitals and research centers should include the full needed information about seizures, marked spikes, patients' MRI and detailed medical diagnoses reports.

Moreover, the effect of electrodes number on the performance of source localization algorithm can be explored for acquired data from different patients and different electrode sensors set. It would be beneficial cost wise to reduce the number of used electrode sensors for EEG recording, hence, different techniques can be used to select the channels that will result in a more accurate source localization with less computational and processing time.

Nonetheless, it is important and interesting to estimate lesions size. This can be done by improving the inverse algorithm so it will be more accurate and less blurred.

Furthermore, new brain source localization algorithms can be applied to the clinical data based on sLORETA and SAFFIRE results in order to get a higher spatial resolution.

Since EEG provides high temporal resolution and fMRI provides excellent spatial resolution, integrating EEG and fMRI will be a good step in order to provide a more accurate source localization that could not be achieved with either imaging technique alone.

References

[1] T. Dierks *et al.*, "Spatial pattern of cerebral glucose metabolism (PET) correlates with localization of intracerebral EEG-generators in Alzheimer's disease," *Clinical Neurophysiology*, vol. 111, no. 10, pp. 1817-1824, 10/1/ 2000.

[2] S. Baillet, J. C. Mosher, and R. M. Leahy, "Electromagnetic brain mapping," *IEEE Signal Processing Magazine*, vol. 18, no. 6, pp. 14-30, 2001.

[3] C. P. Panayiotopoulos, A clinical guide to epileptic syndromes and their treatment, Rev. 2nd ed. ed. London:: Springer-Verlag, 2010.

[4] J. W. Miller, H. P. Goodkin, S. Dickinson, and B. W. Abou-Khalil, *Epilepsy*. Chichester, England: Wiley, 2014.

[5] S. Zubkov and D. Friedman, "Epilepsy treatment and creativity," *Epilepsy & Behavior*, vol. 57, Part B, pp. 230-233, 2016.

[6] N. Akalan, C. Di Rocco, and SpringerLink, *Pediatric Epilepsy Surgery*. Vienna: Springer Vienna, 2012.

[7] M. A. Phyllis Porter. Early Brain Development [Online]. Available: http://www.educarer.org/brain.htm

[8] O. Sporns, Networks of the brain, Cambridge, Mass. :: MIT Press, 2011.

[9] I. O. Tanzer, "Numerical modeling in electro-and magnetoencephalography," 2006.

[10] M. J. Brodie, S. C. Schachter, P. Kwan, and I. Ebrary, *Epilepsy*. Health Press Ltd, 2012.

[11] J. Engel Jr, "Introduction to temporal lobe epilepsy," *Epilepsy Research*, vol. 26, no. 1, pp. 141-150, 1996.

[12] K. K. Oguz, "Magnetic Resonance Imaging in Epilepsy," in *Pediatric Epilepsy Surgery*, N. Akalan and C. Di Rocco, Eds. Vienna: Springer Vienna, pp. 61-83, 2012.

[13] A. D. Elster and W. Mirza, "MR imaging in chronic partial epilepsy: role of contrast enhancement," *American Journal of Neuroradiology*, vol. 12, no. 1, pp. 165-70, January 1, 1991.

[14] H. Pardoe and R. Kuzniecky, "Advanced Imaging Techniques in the Diagnosis of Nonlesional Epilepsy: MRI, MRS, PET, and SPECT," *EPILEPSY CURRENTS*, vol. 14, no. 3, pp. 121-124, 2014.

[15] H. Urbach and SpringerLink, *MRI in Epilepsy*. Berlin, Heidelberg: Springer Berlin Heidelberg, 2013.

[16] J. A. Detre, "fMRI: Applications in epilepsy," *EPILEPSIA*, vol. 45, no. s4, pp. 26-31, 2004.

[17] S. Ogawa *et al.*, "Functional brain mapping by blood oxygenation level-dependent contrast magnetic resonance imaging. A comparison of signal characteristics with a biophysical model," *Biophysical Journal*, vol. 64, no. 3, pp. 803-812, 1993.

[18] M. A. Griswold *et al.*, "Resolution enhancement in single-shot imaging using simultaneous acquisition of spatial harmonics (SMASH)," (in Eng), *Magn Reson Med*, vol. 41, no. 6, pp. 1236-45, Jun 1999.

[19] J. A. Detre, J. I. Sirven, D. C. Alsop, M. J. O'Connor, and J. A. French, "Localization of subclinical ictal activity by functional magnetic resonance imaging: correlation with invasive monitoring," (in Eng), *Ann Neurol*, vol. 38, no. 4, pp. 618-24, Oct 1995.

[20] J. A. Detre, D. C. Alsop, G. K. Aguirre, and M. R. Sperling, "Coupling of cortical and thalamic ictal activity in human partial epilepsy: demonstration by functional magnetic resonance imaging," (in Eng), *Epilepsia,* vol. 37, no. 7, pp. 657-61, Jul 1996.

[21] J. R. Ives, S. Warach, F. Schmitt, R. R. Edelman, and D. L. Schomer, "Monitoring the patient's EEG during echo-planar MRI," *Electroencephalography and Clinical Neurophysiology,* vol. 87, no. 6, pp. 417-420, 12// 1993.

[22] P. J. Allen, G. Polizzi, K. Krakow, D. R. Fish, and L. Lemieux, "Identification of EEG events in the MR scanner: the problem of pulse artifact and a method for its subtraction," (in Eng), *Neuroimage,* vol. 8, no. 3, pp. 229-39, Oct 1998.

[23] P. J. Allen, O. Josephs, and R. Turner, "A method for removing imaging artifact from continuous EEG recorded during functional MRI," *Neuroimage,* vol. 12, no. 2, pp. 230-9, Aug 2000.

[24] A. Hoffmann, L. Jager, K. J. Werhahn, M. Jaschke, S. Noachtar, and M. Reiser, "Electroencephalography during functional echo-planar imaging: detection of epileptic spikes using post-processing methods," *Magn Reson Med,* vol. 44, no. 5, pp. 791-8, Nov 2000.

[25] A. Salek-Haddadi, K. J. Friston, L. Lemieux, and D. R. Fish, "Studying spontaneous EEG activity with fMRI," (in Eng), *Brain Res Brain Res Rev,* vol. 43, no. 1, pp. 110-33, Sep 2003.

[26] A. Salek-Haddadi, L. Lemieux, M. Merschhemke, K. J. Friston, J. S. Duncan, and D. R. Fish, "Functional magnetic resonance imaging of human absence seizures," *Ann Neurol,* vol. 53, no. 5, pp. 663-7, May 2003.

[27] J. Gotman, "Epileptic networks studied with EEG-fMRI," (in Eng), *Epilepsia,* vol. 49 Suppl 3, pp. 42-51, 2008.

[28] E. Formaggio, S. F. Storti, A. Bertoldo, P. Manganotti, A. Fiaschi, and G. M. Toffolo, "Integrating EEG and fMRI in epilepsy," *NEUROIMAGE,* vol. 54, no. 4, pp. 2719-2731, 2011.

[29] A. S. Harvey, "Temporal lobe epilepsy in childhood," Ph.D, University of Melbourne, 1993.

[30] C. la Fougère, A. Rominger, S. Förster, J. Geisler, and P. Bartenstein, "PET and SPECT in epilepsy: A critical review," *Epilepsy & Behavior,* vol. 15, no. 1, pp. 50-55, 2009.

[31] R. D. Neirinckx *et al.*, "Technetium-99m d,l-HM-PAO: a new radiopharmaceutical for SPECT imaging of regional cerebral blood perfusion," *J Nucl Med,* vol. 28, no. 2, pp. 191-202, Feb 1987.

[32] W. Van Paesschen, "Ictal SPECT," *Epilepsia,* vol. 45 Suppl 4, pp. 35-40, 2004.

[33] M. R. Newton, S. F. Berkovic, M. C. Austin, C. C. Rowe, W. J. McKay, and P. F. Bladin, "Postictal switch in blood flow distribution and temporal lobe seizures," *J Neurol Neurosurg Psychiatry,* vol. 55, no. 10, pp. 891-4, Oct 1992.

[34] S. Weil, S. Noachtar, S. Arnold, T. A. Yousry, P. A. Winkler, and K. Tatsch, "Ictal ECD-SPECT differentiates between temporal and extratemporal epilepsy: confirmation by excellent postoperative seizure control," *Nucl Med Commun,* vol. 22, no. 2, pp. 233-7, Feb 2001.

[35] M. V. Spanaki, S. S. Spencer, M. Corsi, J. MacMullan, J. Seibyl, and I. G. Zubal, "Sensitivity and specificity of quantitative difference SPECT analysis

in seizure localization," (in Eng), *J Nucl Med*, vol. 40, no. 5, pp. 730-6, May 1999.

[36] M. D. Devous, Sr., R. A. Thisted, G. F. Morgan, R. F. Leroy, and C. C. Rowe, "SPECT brain imaging in epilepsy: a meta-analysis," *J Nucl Med*, vol. 39, no. 2, pp. 285-93, Feb 1998.

[37] J. J. Zaknun *et al.*, "Comparative analysis of MR imaging, ictal SPECT and EEG in temporal lobe epilepsy: a prospective IAEA multi-center study," (in Eng), *Eur J Nucl Med Mol Imaging*, vol. 35, no. 1, pp. 107-15, Jan 2008.

[38] R. A. Avery *et al.*, "Decreased cerebral blood flow during seizures with ictal SPECT injections," *Epilepsy Research*, vol. 40, no. 1, pp. 53-61, 2000.

[39] M. T. Madsen, "Recent Advances in SPECT Imaging," *The Journal of Nuclear Medicine*, vol. 48, no. 4, pp. 661-673, 2007.

[40] M. Rossman, M. Adjouadi, M. Ayala, and I. Yaylali, "An interactive interface for seizure focus localization using SPECT image analysis," *Computers in Biology and Medicine*, vol. 36, no. 1, pp. 70-88, 2006.

[41] I. Sarikaya, "PET studies in epilepsy," (in Eng), *Am J Nucl Med Mol Imaging*, vol. 5, no. 5, pp. 416-30, 2015.

[42] R. C. Knowlton and J. Shih, "Magnetoencephalography in Epilepsy," *Epilepsia (Series 4)*, Article vol. 45, pp. 61-71, 2004.

[43] M. Lau, D. Yam, and J. G. Burneo, "A systematic review on MEG and its use in the presurgical evaluation of localization-related epilepsy," *Epilepsy Research*, vol. 79, no. 2–3, pp. 97-104, 2008.

[44] X. De Tiège *et al.*, "Recording epileptic activity with MEG in a light-weight magnetic shield," *Epilepsy Research*, vol. 82, no. 2–3, pp. 227-231, 12// 2008.

[45] R. C. Knowlton, "The role of FDG-PET, ictal SPECT, and MEG in the epilepsy surgery evaluation," *Epilepsy and Behavior*, vol. 8, no. 1, pp. 91-101, 2006.

[46] K. Kaiboriboon, H. O. Luders, M. Hamaneh, J. Turnbull, and S. D. Lhatoo, "EEG source imaging in epilepsy-practicalities and pitfalls,"*Nature Reviews Neurology*", vol. 8, no. 9, pp. 498-507, 2012.

[47] M. Hämäläinen, R. Hari, R. J. Ilmoniemi, J. Knuutila, and O. V. Lounasmaa, "Magnetoencephalography—theory, instrumentation, and applications to noninvasive studies of the working human brain,"*Reviews of Modern Physics"*, vol. 65, no. 2, pp. 413-497, 1993.

[48] C. M. Michel, M. M. Murray, G. Lantz, S. Gonzalez, L. Spinelli, and R. Grave de Peralta, "EEG source imaging," *Clinical neurophysiology : official journal of the International Federation of Clinical Neurophysiology*, vol. 115, no. 10, pp. 2195-222, 2004.

[49] T. Zarghami, H. S. Mir, and H. Al-Nashash, "Calibration of Low Density EEG Sensor Arrays for Brain Source Localization," in *Neural Information Processing: 19th International Conference, ICONIP 2012, Doha, Qatar, November 12-15, 2012, Proceedings, Part I*, T. Huang, Z. Zeng, C. Li, and C. S. Leung, Eds. Berlin, Heidelberg: Springer Berlin Heidelberg, pp. 331-338, 2012.

[50] J. C. Mosher and R. M. Leahy, "Source Localization Using Recursively Applied and Projected (RAP) MUSIC," *IEEE Transactions on Signal Processing*, vol. 47, no. 2, pp.3, 1999.

[51] D. Cheyne and J. Verba, "Biomagnetism," in *Encyclopedia of Medical Devices and Instrumentation*: John Wiley & Sons, Inc., 2006.

[52] V. Murzin, A. Fuchs, and J. A. Scott Kelso, "Detection of correlated sources in EEG using combination of beamforming and surface Laplacian methods," *Journal of Neuroscience Methods,* vol. 218, no. 1, pp. 96-102, 2013.

[53] I. S. Mohamed *et al.*, "Source localization of interictal spike-locked neuromagnetic oscillations in pediatric neocortical epilepsy," *Clinical neurophysiology : official journal of the International Federation of Clinical Neurophysiology,* vol. 124, no. 8, pp. 1517-27, 2013.

[54] M. A. Jatoi, N. Kamel, A. S. Malik, I. Faye, and T. Begum, "A survey of methods used for source localization using EEG signals," *Biomedical Signal Processing and Control,* vol. 11, pp. 42-52, 2014.

[55] H. Liu, P. H. Schimpf, G. Dong, X. Gao, F. Yang, and S. Gao, "Standardized shrinking LORETA-FOCUSS (SSLOFO): a new algorithm for spatio-temporal EEG source reconstruction," *IEEE Trans Biomed Eng,* vol. 52, no. 10, pp. 1681-91, Oct 2005.

[56] M. Popescu, S. D. Blunt, and T. Chan, "Magnetoencephalography source localization using the source affine image reconstruction (SAFFIRE) algorithm," *IEEE Trans Biomed Eng,* vol. 57, no. 7, pp. 1652-62, Jul 2010.

[57] W. Penny and K. Friston, "Functional imaging," *Scholarpedia,* vol. 2, p. 1478, 2007.

[58] R. Henson, "Multi-modal Face Dataset," W. T. C. f. Neuroimaging, Ed., ed, 2003.

[59] E. Callaway, *Brain electrical potentials and individual psychological differences*. Grune & Stratton, 1975.

[60] T. Allison, A. Puce, D. D. Spencer, and G. McCarthy, "Electrophysiological studies of human face perception. I: Potentials generated in occipitotemporal cortex by face and non-face stimuli," *Cereb Cortex,* vol. 9, no. 5, pp. 415-30, Jul-Aug 1999.

[61] S. Bentin, T. Allison, A. Puce, E. Perez, and G. McCarthy, "Electrophysiological Studies of Face Perception in Humans," *Journal of cognitive neuroscience,* vol. 8, no. 6, pp. 551-565, 1996.

[62] N. George, J. Evans, N. Fiori, J. Davidoff, and B. Renault, "Brain events related to normal and moderately scrambled faces," *Brain Res Cogn Brain Res,* vol. 4, no. 2, pp. 65-76, Sep 1996.

[63] B. Jemel, M. Pisani, M. Calabria, M. Crommelinck, and R. Bruyer, "Is the N170 for faces cognitively penetrable? Evidence from repetition priming of Mooney faces of familiar and unfamiliar persons," *Cognitive Brain Research,* vol. 17, no. 2, pp. 431-446, 7/15/ 2003.

[64] N. Ille, P. Berg, and M. Scherg, "Artifact correction of the ongoing EEG using spatial filters based on artifact and brain signal topographies," *J Clin Neurophysiol,* vol. 19, no. 2, pp. 113-24, Apr 2002.

[65] M. Hassan *et al.*, "Identification of Interictal Epileptic Networks from Dense-EEG," *Brain Topogr,* vol. 30, no. 1, pp. 60-76, Jan 2017.

[66] A. Sohrabpour, Y. Lu, P. Kankirawatana, J. Blount, H. Kim, and B. He, "Effect of EEG electrode number on epileptic source localization in pediatric patients," *Clin Neurophysiol,* vol. 126, no. 3, pp. 472-80, Mar 2015.

[67] M. I. Al-Kadi, M. B. Reaz, M. A. Ali, and C. Y. Liu, "Reduction of the dimensionality of the EEG channels during scoliosis correction surgeries using a wavelet decomposition technique," *Sensors (Basel),* vol. 14, no. 7, pp. 13046-69, Jul 21 2014.

Vita

Wisal Elfatih Mohamed Siyam was born in 1990, in Abu Dhabi, United Arab Emirates. She received her primary and preparatory education in Abu Dhabi and graduated from Saad's High school in Sudan in 2008. Ms. Siyam joined the University of Khartoum in 2008 and graduated in the year 2013 with a Bachelor's degree in Electrical and Electronics Engineering. From 2013 to 2014, she worked as teaching assistant in the University of Khartoum and then as a Software Testing Engineer in Banan IT services from 2014 to 2015.

She was granted a teaching assistantship in order to pursue a Master's program in Electrical Engineering at the American University of Sharjah in 2015. Her research interests are in signal processing and biomedical engineering.